

Ismael Ribeiro de Assis

**From the Keldysh formalism to the Boltzmann
equation for spin drift and diffusion**

Uberlândia, Minas Gerais, Brasil

29 de julho de 2019

Ismael Ribeiro de Assis

**From the Keldysh formalism to the Boltzmann equation
for spin drift and diffusion**

Dissertação apresentada ao Programa de Pós-graduação em Física da Universidade Federal de Uberlândia, como requisito parcial para obtenção do título de mestre em Física Teórica. Área de Concentração: Física da Matéria Condensada.

Universidade Federal de Uberlândia – UFU

Instituto de Física - INFIS

Programa de Pós-Graduação

Orientador: Prof. Dr. Gerson Ferreira Junior

Uberlândia, Minas Gerais, Brasil

29 de julho de 2019

Ficha Catalográfica Online do Sistema de Bibliotecas da UFU
com dados informados pelo(a) próprio(a) autor(a).

A848 Assis, Ismael Ribeiro de, 1994-
2019 From the Keldysh formalism to the Boltzmann equation for spin
drift and diffusion [recurso eletrônico] / Ismael Ribeiro de Assis. -
2019.

Orientador: Gerson Ferreira Júnior.
Dissertação (Mestrado) - Universidade Federal de Uberlândia,
Pós-graduação em Física.
Modo de acesso: Internet.
Disponível em: <http://dx.doi.org/10.14393/ufu.di.2019.2247>
Inclui bibliografia.

1. Física. I. Ferreira Júnior, Gerson , 1982-, (Orient.). II.
Universidade Federal de Uberlândia. Pós-graduação em Física. III.
Título.

CDU: 53

Bibliotecários responsáveis pela estrutura de acordo com o AACR2:
Gizele Cristine Nunes do Couto - CRB6/2091
Nelson Marcos Ferreira - CRB6/3074



SERVIÇO PÚBLICO FEDERAL
MINISTÉRIO DA EDUCAÇÃO
UNIVERSIDADE FEDERAL DE UBERLÂNDIA
INSTITUTO DE FÍSICA
PROGRAMA DE PÓS-GRADUAÇÃO EM FÍSICA



ISMAEL RIBEIRO DE ASSIS

Dissertação apresentada ao Programa de Pós-graduação em Física, do Instituto de Física, da Universidade Federal de Uberlândia, como requisito parcial para obtenção do título de Mestre em Física.

Uberlândia, 29 de julho de 2019.

BANCA EXAMINADORA

Prof. Dr. Gerson Ferreira Junior
Universidade Federal de Uberlândia - UFU

Dr. George Balster Martins
Universidade Federal de Uberlândia - UFU

Prof. Dr. Antonio Carlos Ferreira Seridonio
Universidade Estadual Paulista - UNESP

Dedico à minha família

Acknowledgements

Gostaria de agradecer as pessoas próximas que fazem com que minha carreira seja possível. Especialmente minha família, minha mãe June, meu pai Anísio e minha irmã Geovana, que durante os anos desta jornada tem me apoiado emocionalmente e financeiramente. Gostaria de agradecer minha namorada Giovanna por estar ao meu lado durante todo o mestrado. Aos meus colegas Físicos pelas discussões e pelo apoio. Ao meu orientador Gerson J. Ferreira, pela paciência e pela disposição em me orientar. A todos que de alguma forma durante meus anos de vida contribuíram para que um título de mestre fosse possível.

*It is not knowledge, but the act of learning,
not possession but the act of getting there,
which grants the greatest enjoyment.*

Carl Friedrich Gauss

Resumo

Nesta dissertação estamos interessados, sobretudo, em apresentar um formalismo matemático com intuito de derivar a equação de transporte de Boltzmann com spin (SBTE, do inglês *spin Boltzmann transport equation*). Nosso principal interesse de pesquisa é especificamente fenômenos de relaxação de spin. O mesmo, é fundamental no campo da spintrônica e pode estar relacionado diretamente com o desenvolvimento de tecnologias futuras. A SBTE fornece uma equação de difusão e arrasto que carrega a informação do decaimento de spin. Com objetivo de derivar a equação de transporte de Boltzmann, devemos recorrer a ferramentas matemáticas, viz., o formalismo de Keldysh e funções de Green de não equilíbrio (NEGF). Uma análise rigorosa e um profundo entendimento do formalismo é fundamental para generalizar a equação de Boltzmann para inclusão de spin, mais altas ordens de interação spin-órbita, espalhamento com impurezas, elétrons, fônons, etc. Verifica-se que fomos capazes de compreender o formalismo e derivar uma equação de difusão e arrasto para spin, o que é uma tarefa formidável. Aqui, apresentamos o passos necessários para não só obter tal equação, mas também como incluir outras interações. Também mostramos como aplicar a equação de difusão e arrasto para um regime conhecido como *Persistent Spin Helix* (PSH). No final de nossa pesquisa também conseguimos derivar formalmente uma nova equação de difusão e arrasto de spin para heteroestruturas com duas subbandas ocupadas. Este é um resultado preliminar, no entanto, novo na literatura. Além disso, aplicamos esta equação para um regime conhecido como *Crossed Persistent Spin Helix* (cPSH), no qual cada subbanda é colocada em regimes de PSH ortogonais. Neste caso, encontramos que a dinâmica de cPSH depende da intensidade relativa entre energia de spin-órbita e o alargamento dos estados induzidos pela impureza. Portanto, compreender o formalismo é proveitoso no que se refere a formalizar a dinâmica de PSH para o caso de duas subbandas, ao passo que extensões para novos sistemas e interações adicionais (integrais de colisão) estão agora ao nosso alcance.

Palavras-chave: Formalismo de Keldysh. Equação de transporte de Boltzmann. Persistent Spin Helix.

Abstract

In this dissertation we are mainly interested in presenting a mathematical formalism in order to derive the Spin Boltzmann Transport equation (SBTE). Our preeminent research interest is spintronics, specifically, spin relaxation phenomena. The aforesaid, is a key phenomena in the field of spintronics and could be direct linked to future technology development. The SBTE provides a spin drift-diffusion equation that carries the information about the spin decay. Aiming to derive the Boltzmann Transport equation (BTE), one has to resort to mathematical tools, viz., the Keldysh formalism and Non-equilibrium Green's functions (NEGF). A rigorous analyses and a deep understanding of the formalism, is crucial in order to generalize the BTE to include spin, higher order spin-orbit interactions, scattering from impurities, electrons, phonons, etc. As it turns out, we have been able to master the formalism and deriving the spin drift-diffusion equation, which is a formidable task. We present steps necessary to not only interpret such equation but also to include other types of interactions one might be interested in. We also show how to apply the spin-drift equation to a regime known as the Persistent Spin Helix (PSH). By the end of our research we have also managed to formally derive a novel spin drift-diffusion equation for heterostructures with two occupied subbands. This is a preliminary result, however, new in the literature. In addition, we have applied it to a regime known as crossed Persistent Spin helix (cPSH), for which the subbands are set into orthogonal PSH regimes. In this case we find that the cPSH dynamics depends on the relative intensity between the spin-orbit energy splitting and the impurity induced broadening of the states. Therefore, mastering the formalism paid off by allowing us to formally generalize the PSH dynamics to the two subband problem, whilst further extensions towards novel systems and additional interactions (collision integrals) are now at reach.

Keywords: Keldysh formalism. Boltzmann Transport equation. Persistent Spin Helix.

Contents

1	INTRODUCTION	13
2	DISCUSSIONS AND FORMALISM	17
2.1.	Propagators and Feynman Diagrams	17
2.2.	Propagators	17
2.3.	Quantum Propagators	19
2.4.	More on Green's functions	22
2.5.	An introduction to Feynman Diagrams	24
2.6.	Self-Energy	25
2.7.	Time evolution operators and the closed path formalism	28
2.8.	Green's Function in the Closed Path formalism	30
2.9.	The Keldysh Formalism	32
2.10.	Using Wick's theorem	34
2.11.	Schwinger-Keldysh Space	35
2.12.	Non-equilibrium Dyson equation	38
3	KINETIC EQUATIONS	41
3.1.	Left-right subtracted Dyson's equation	41
3.2.	The Gradient Expansion	42
3.3.	The quasi-particle approximation	44
3.4.	The Boltzmann Equation	45
3.5.	The Quantum Spin Boltzman Equation	47
4	APPLICATIONS AND RESULTS	49
4.1.	2D GaAs Quantum well	49
4.2.	Drift-Diffusion Equations	50
4.3.	Persistent Spin Helix (PSH)	54
4.4.	The drift-diffusion equation for two subbands	57
4.5.	Crossed PSH regime	61
5	CONCLUSIONS	67
	BIBLIOGRAPHY	69

APPENDIX	73
APPENDIX A – BOLTZMANN WEIGHTING FACTOR	75
APPENDIX B – OPERATORS USING CLOSED CONTOUR	77
APPENDIX C – WICK'S THEOREM	81
APPENDIX D – CONVOLUTION RELATION IN THE WIGNER COORDINATES	85

1 Introduction

In this dissertation we present a mathematical formalism in order to derive the Boltzmann transport equation (BTE) and the Spin Boltzmann Transport equation (SBTE). We also show how to use it for some applications and obtain a new result not found in the literature. The BTE assume many forms and for the equilibrium case it's frequently displayed in statistical mechanics and solid state physics books. However, in this dissertation we are interested in non-equilibrium phenomena, such as spin relaxation times, thus, additional mathematical tools have to be implemented.

In kinetic theory one is not interested in the motion of each particle individually, but rather in the distribution function $f_{\mathbf{k}}(\mathbf{r}, \mathbf{k}, t)$, which is a number from 0 to 1. It yields the probability of a particle being in a certain position \mathbf{r} , state \mathbf{k} , at a time t . The distribution function also allows one to compute physical quantities such as the current, particle densities, etc. Therefore, determining the BTE means we're asking the question: given a state \mathbf{k} what's the probability, i.e. the distribution function $f_{\mathbf{k}}$, of being occupied? If an external force \mathbf{F} drives the particle to move with a velocity \mathbf{v} and there's no scattering, it will follow a certain trajectory in phase space. If one knows the probability in a state earlier, it will follow along the trajectory, hence

$$f_{\mathbf{k}}(\mathbf{r}, \mathbf{k}, t) = f_{\mathbf{k}}(\mathbf{r} - \mathbf{v}dt, \mathbf{k} - \mathbf{F}dt, t + dt), \quad (1.1)$$

i.e., the probability doesn't change,

$$\frac{df_{\mathbf{k}}}{dt} = 0. \quad (1.2)$$

Applying the chain rule one finds

$$\frac{\partial f_{\mathbf{k}}}{\partial t} + \mathbf{v} \cdot \nabla_{\mathbf{r}} f_{\mathbf{k}} + \mathbf{F} \cdot \nabla_{\mathbf{k}} f_{\mathbf{k}} = 0, \quad (1.3)$$

where \mathbf{v} is the velocity and \mathbf{F} the external force. Eq.(1.3) is the collisionless Boltzmann equation. The left-hand side is responsible for drift and diffusion terms. The distribution function must obey this equation, for the classical case with no external force the solution is the Maxwell-Boltzmann distribution (HUANG, 1987) and for the quantum case the Fermi-Dirac distribution function (PATHRIA; BEALE, 2011).

On the other hand, for an electron following a certain trajectory in phase space in a system out of equilibrium, the probability of being in that state could change by plenty of things, e.g., one might shine light into the material, thus, the photons increase the probability of this or another state being occupied, the electron might scatter of the

trajectory by an impurity or another electron, it can recombine with a hole and disappear, etc. Hence, to describe this kind of system, all relevant possibilities have to be accounted and Eq.(1.3) needs a correction, namely

$$\frac{\partial f_{\mathbf{k}}}{\partial t} + \mathbf{v} \cdot \nabla_{\mathbf{r}} f_{\mathbf{k}} + \mathbf{F} \cdot \nabla_{\mathbf{k}} f_{\mathbf{k}} = I_{\mathbf{k}}. \quad (1.4)$$

On right-hand side we have included what is known as the collision integral. It is responsible for interactions and scattering. Our task is to include spin in the left-hand side of Eq.(1.4) and to build a proper collision integral to fit the phenomena we are interested in.

For a system out of equilibrium, to include quantum effects, one has to resort to the non-equilibrium Green's functions technique (NEGF). We introduce the Green's functions, also known as propagators, in the second chapter along with how we can portray them in a pictorial and intuitive way as Feynman diagrams. This mathematical machinery, in a very elegant way, accounts for all the possibilities an electron might scatter off. This introduction is meant to be a pedagogical one, we do not actually use Feynman diagrams up to chapter 3, however, we show how to use them and the meaning of propagators. Such concepts are often overlooked in introductory texts.

We also show that the Green's functions are not enough and introduce the so-called closed path and Keldysh formalisms. With such tools one is able to write the famous Dyson equation in what is known as the Schwinger-Keldysh space, leading to the Kinetic equations. In chapter 3 we derive the BTE and SBTE using the standard recipe, by changing to the Wigner coordinates and applying the gradient expansion.

The possible applications of this formalism and the BTE range from plasma physics, fluid dynamics to economics (RICHMOND; MIMKES; HUTZLER, 2013). Nevertheless, in chapter 4 it's where it all converge to our main research field of interest, spintronics.

Spintronics is a key field in the quest for smaller and faster devices. After revolutionizing the world by building technology that rely in one of the electron's charge, e.g., the transistor, we now turn to the spin. Understanding and controlling it, is fundamental for future spintronic devices and quantum computing.

Perhaps one of the most notorious life changing application of spintronics is the discovery of the giant magnetoresistance (GMR) by Albert Fert and Peter Grünberg (FERT, 2008) (GRÜNBERG, 2008) which they were awarded with the Nobel prize in 2007 for it. Their research along the creation of "spin valve" by the IBM researcher Stuart Parkin increased drastically the storage capacity of hard disks (DIENY et al., 1991). As future perspectives of spintronics applications, the most promising is the potential to build quantum bits (qubits) which are superposition of many spin states entangled. This is the basis for quantum information processing and specifically, for building a spin-based

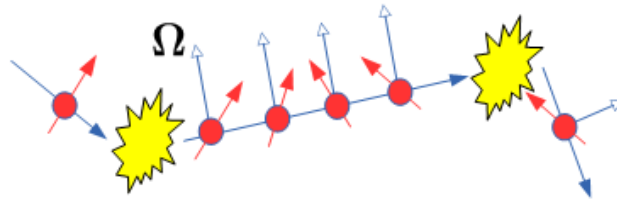


Figure 1 – Illustration of the Dyakonov-Perel relaxation mechanism. Spin (red arrow) precessing about a precession vector Ω , which is defined by the spin-orbit coupling, thus depending on the direction of motion given by the momentum \mathbf{k} . At scattering events, the direction of motion changes, thus changing Ω , which becomes a random variable after multiple scatterings.

quantum computer.

An electron moving through the conduction band is not held by strong nuclear interactions, however, it will be affected by external or internal electrical fields, such as the one created by conduction band discontinuities. In this thesis, we have in mind III-V semiconductor heterostructures, these feature a crystallographic inversion asymmetry also inducing an electrical field. These fields yield spin-orbit interactions, namely, Rashba (RASHBA, 1960) and Dresselhaus (DRESSELHAUS, 1955).

Spintronics is a vast field of study that could be essential for future technology. Controlling spin would be great, but it has a catch. Spin states have life times, as we shall see. If on the one hand the spin-orbit coupling helps to control the spin, on the other hand, it is impractical to transport spin over long distances (KOHDA; SALIS, 2017). Spin orbit interactions act like an effective magnetic field, which depends upon the wave vector of the electron. The spin precesses about a vector precession Ω created by the effective magnetic field. The spin evolves in time with

$$\frac{d\langle\sigma\rangle}{dt} = \frac{i}{\hbar}[H^{soc}, \langle\sigma\rangle] = \Omega \times \langle\sigma\rangle, \quad (1.5)$$

where H^{soc} is the spin-orbit Hamiltonian and the vector $\Omega = \frac{\alpha}{\hbar}(-\mathbf{k}_y, \mathbf{k}_x, 0)$, considering only the Rashba interaction for now.

If the direction of the effective magnetic field changes, say by scattering as Figure 1, the axis about which the spin precesses upon, changes direction along with the field and the precession frequency, leading to a spin relaxation, namely, Dyakonov-Perel.

The main mechanisms responsible for such phenomena, are the D'yakonov-Perel and Elliot-Yafet. The relaxation time of the D'yakonov Perel mechanism is presented in chapter 4. The Elliot-Yaffet mechanics is not derived in this thesis, however it is an extension of the formalism presented.

Another beautiful phenomena caused by spin orbit interaction is the Persistent

Spin Helix (PSH) ([BERNEVIG; ORENSTEIN; ZHANG, 2006](#)), discussed in chapter 4. There, the Rashba and Dresselhaus spin-orbit interactions combine to define effective spin operators that commute with the Hamiltonian, thus, leading to a conservation rule. This fine tuning leads to a long lived spin helix with well defined spin wave patterns. The robustness of the PSH against scattering events, might lead to robust implementations of the Datta-Das spin transistor ([DATTA; DAS, 1990](#); [SCHLIEMANN; EGUES; LOSS, 2003](#)).

In chapter 2 and 3 we present the formalism necessary to derive the kinetic equations. Then, in chapter 4 we pursue the spin drift-diffusion equation and apply it to the PSH regime. To wrap it up, we exhibit the result accomplished by our research using the tools mastered writing this dissertation. We have developed a formal derivation of the spin drift-diffusion equation for two subbands, allowing us to analyze the regime of crossed Persistent Spin Helix (cPSH).

2 Discussions and Formalism

2.1. Propagators and Feynman Diagrams

The following sections are meant as an introduction to the non-equilibrium Green's Functions method and Feynman Diagrams, a first look at this exciting field. Looking at the non-equilibrium expansion and deriving the general kinetic equation in the literature, might seem scary, and indeed a solid background on Green's functions and Feynman diagrams is needed. Very important concepts are introduced without going further into the details, although, passing on the general idea behind all the harsh math of non-equilibrium systems. In the general literature there's necessity of a very well deserved discussion about the meaning of propagators rather than just writing the relation between all of its forms, hence sections 2.2 and 2.3 . The discussion about Feynman Diagrams, a general many-body diagram is used, i.e., we do not use the usual topology of the vast array of diagrams, but instead we use their meaning. The self-energy concept is very important, specially when deriving key equations, although, a background on Feynman diagrams is crucial for a deep understanding. We chose to give a comprehensive discussion about it, giving the general idea, so that further in the future, the self-energy is not just "math" and an interested reader can understand what is actually going on.

2.2. Propagators

The main system we are illustrating, is of a particle moving through a semiconductor. Describing accurately, can be extremely hard, because it involves computing the interaction between one particle with infinity of others.

A particle moving through a system, pushes or pulls another ones by Coulomb interaction, becoming surrounded by them, the result is what we call a "quasi-particle". A sort of cloud of particles, behaving collectively, producing a phenomena, although seemly like an individual particle. For instance

1. Phonons - Waves in crystal lattice of a solid;
2. Magnons - Fluctuations in the density of spin angular momentum, i.e "spin waves";
3. Hole - "An empty space" in a crystal lattice with positive charge, usually in the valence band of a semiconductor. Etc.

Due to this collective behavior, quasi-particles have effective mass and life times. One can ask, how can we calculate their physical properties? The answer is propagators! Fortunately, to have important information about the physical properties of the system we do not have to estimate the behavior of each individual particle*, but rather the average behavior of one or two particles. Those averages are called *one-particle propagator* and *two-particle propagator*.

To understand what a propagator is, think for now the electron moving in a semiconductor system as classical (in other words, one ball colliding with another). The idea behind it, is this: A particle is placed at point \mathbf{r}_1 at a time t_1 , let it move throughout the system. The propagator is the probability (in the quantum case, the probability amplitude) to find the particle at point \mathbf{r}_2 and time t_2 .

Propagators yields most physical features of the system in a very intuitively way. There are a few methods to calculate them (MATTUCK, 1992), the main one consists in expanding the propagator in a series of integrals and evaluating approximately. This is done in a very elegant way using *Feynman Diagrams*.

Semiconductors are a set of positively charged ions with some irregularities called impurities, an electron moving through the system has to go from point A to B. There are infinity ways it can do that. It can either move freely, or interact one, two, infinity times with an impurity. Consider some of the possibilities. Figure 2 represents some of the ways an electron might go from point A to point B in a crystal. Define the probability to move freely $P_0(A, B)$.

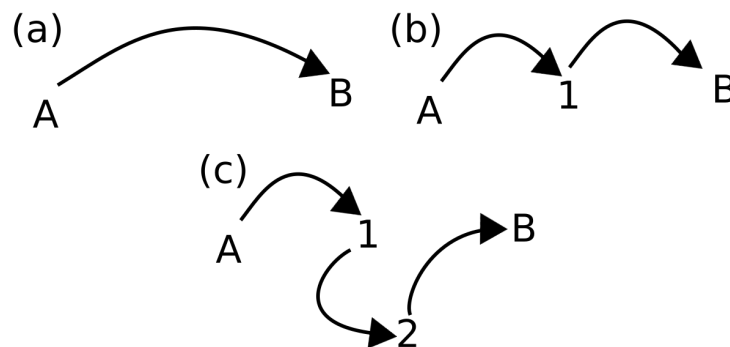


Figure 2 – Possible ways a particle can propagate from point A to point B. a) The particle propagates without being scattered by an impurity. b) The particle is scattered once by an impurity before getting to point B. c) The particle is scattered twice by an impurity before getting to point B.

Now consider an electron propagating from point A to B, but interacting with an impurity at point 1 along the way, as depicted in figure 2. The particle propagates

*The name “particle” is used, but essentially we’re taking about particle or quasi-particles, as we’ve seen, they are by all means, particles!

freely up until point 1, where the impurity is placed. Call this probability $P_0(A, 1)$. There's the probability of actually interacting with the impurity, define it $P(1)$. Then it propagates freely to point B, call this probability $P_0(1, B)$. Therefore, the total probability of an electron moving through this exactly path and interacting with the impurity is $P(A, B) = P_0(A, 1)P(1)P_0(1, B)$.

Consider again an electron going from point A to B, but this time two impurities are placed in points 1 and 2. It can propagate freely, interact with impurity 1 and 2 individually or it can interact with both as depicted in figure 2. Therefore, the probability of doing this exactly path and interacting with 1 and then 2 is $P(A, B) = P_0(A, 1)P(1)P_0(1, 2)P(2)P_0(2, B)$.

The electron being scattered twice, yields the total probability of ways to propagate from point A to B

$$P(A, B) = P_0(A, B) + P_0(A, 1)P(1)P_0(1, B) + P_0(A, 2)P(2)P_0(2, B) \\ + P_0(A, 1)P(1)P_0(1, 2)P(2)P_0(2, B) + P_0(A, 2)P(2)P_0(2, 1)P(1)P_0(1, B).$$

A propagator accounts the probability of all possibles ways a particle can go from point A to B, therefore, in a system with N scattering events, the total probability is

$$P(A, B) = P_0(A, B) + P_0(A, 1)P(1)P_0(1, B) + P_0(A, 2)P(2)P_0(2, B) + \dots \\ + P_0(A, N)P(N)P_0(N, B) + P_0(A, 1)P(1)P_0(1, 2)P(2)P_0(2, B) + \dots \\ + P_0(A, 1)P(1)P_0(1, N)P(N)P_0(N, B) + \dots + P_0(A, 2)P(2)P_0(2, N)P(N)P_0(N, B). \quad (2.1)$$

which is a infinite series. If one is not considering a classical system, the term “probability” is mistakenly used, we have actually to compute the probability amplitude instead.

The problem looks unsolvable, we have to deal with infinity possibilities, but us physicists get our way around it. This is the very soul of the physics behind the description of particles moving in semiconductors. We shall see in the next sections that the propagator actually have another name, *Green's Function* and the probabilities are an infinity string of integrals which can be portrayed as Feynman diagrams providing an intuitively way to describe complicated systems.

2.3. Quantum Propagators

In this section we shall not consider the electron moving in a metal system as classical, but instead, we finally start looking at it as a quantum object.

Quantum propagators actually have another name, Green's Functions. One is familiar with the Green's Functions method in solving differential equations, that will

soon be employed[†]. These functions have a deeper statistical meaning, often overlooked. From Eq. 2.1, consider only two processes, i.e, the electron can move solely by two ways, call the probability (classical) $P_0(A, B) = P_0$ and $P_0(A, 1)P(1)P_0(1, B) = P_1$, thus the total probability P is

$$P = P_0 + P_1. \quad (2.2)$$

We also define the total probability amplitude as G as

$$G = G_0 + G_1. \quad (2.3)$$

The total probability is related to the probability amplitude as

$$P = G^*G = |G_0|^2 + |G_1|^2 + G_0^*G_1 + G_1^*G_0, \quad (2.4)$$

where last two terms are interference terms, hence, in the quantum case the total probability isn't just the sum of probabilities.

Quantum propagators are also called Green's functions, a first glance at them, one can get lost due to what it seems infinity relations among these functions*. These propagators that we are going to be dealing with, have their roots as probabilities amplitudes of a particle moving certain paths. One can get lost about their meaning since they come in all forms and shapes, leading to many Green's functions relations. Next we define some of the these relations that will be used through out the entire thesis.

There are several ways to write Green's functions. The one that will play a fundamental role to write a non-equilibrium expansion is called causal or average Green's function

$$G(\mathbf{r}, t, \mathbf{r}', t') = -i \left\langle T \psi_{\mathcal{H}}(\mathbf{r}, t) \psi_{\mathcal{H}}^\dagger(\mathbf{r}', t') \right\rangle, \quad (2.5)$$

where the ψ 's are field operators in the Heisenberg picture. T is called the time ordering operator, it rearranges the field operators so that the time decrease from left to right, where no times are equal. Namely for general time-dependent operators \hat{A} and \hat{B}

$$T(\hat{A}(t)\hat{B}(t')) = \begin{cases} \hat{A}(t)\hat{B}(t'), & t > t', \\ \mp \hat{B}(t')\hat{A}(t), & t' > t. \end{cases} \quad (2.6)$$

The time ordering symbol also rearranges field operators, as for equal time the $\psi_{\mathcal{H}}^\dagger$'s are placed to the left and $\psi_{\mathcal{H}}$'s to the right. The minus sign for fermions always appears when two field operators are interchanged (BRUUS; FLENSBERG, 2004).

The average Green's function can also be written

$$G(\mathbf{r}, t, \mathbf{r}', t') = \begin{cases} G^<(\mathbf{r}, t, \mathbf{r}', t') & t' > t \\ G^>(\mathbf{r}, t, \mathbf{r}', t') & t > t' \end{cases}. \quad (2.7)$$

[†]We shall use it to solve the Schöndiger equation

*For a pedagogical introduction to Green's functions see (ODASHIMA; PRADO; VERNEK, 2017)

$G^>$ and $G^<$ are the so-called *greater* and *lesser* Green's functions respectively. In second quantization they are written

$$G^>(\mathbf{r}, t, \mathbf{r}', t') = -i \langle \psi_{\mathcal{H}}(\mathbf{r}, t) \psi_{\mathcal{H}}^\dagger(\mathbf{r}', t') \rangle, \quad (2.8)$$

$$G^<(\mathbf{r}, t, \mathbf{r}', t') = -i(\pm 1) \langle \psi_{\mathcal{H}}^\dagger(\mathbf{r}', t') \psi_{\mathcal{H}}(\mathbf{r}, t) \rangle. \quad (2.9)$$

Dealing with non-equilibrium problems another function is commonly used in the literature (RAMMER, 2007), the anti-time-ordered Green's function, defined as

$$\tilde{G}(\mathbf{r}, t, \mathbf{r}', t') = -i \langle \tilde{T} \psi_{\mathcal{H}}(\mathbf{r}, t) \psi_{\mathcal{H}}^\dagger(\mathbf{r}', t') \rangle, \quad (2.10)$$

where \tilde{T} is the anti-time ordering operator, it acts as the opposite of T . Hence

$$\tilde{G}(\mathbf{r}, t, \mathbf{r}', t') \begin{cases} G^<(\mathbf{r}, t, \mathbf{r}', t') & t > t' \\ G^>(\mathbf{r}, t, \mathbf{r}', t') & t' > t. \end{cases} \quad (2.11)$$

There's also a second type of Green's Functions called *Retarded* and *Advanced*, they are defined as

$$G^R(\mathbf{r}, t, \mathbf{r}', t') = -i\theta(t - t') \langle [\psi(\mathbf{r}, t), \psi^\dagger(\mathbf{r}', t')]_{\pm} \rangle, \quad (2.12)$$

where $+$ sign represents the commutator for bosons and $-$ the anti-commutator for fermions. Analogously the advanced Green's functions

$$G^A(\mathbf{r}, t, \mathbf{r}', t') = i\theta(t' - t) \langle [\psi_{\mathcal{H}}(\mathbf{r}, t), \psi_{\mathcal{H}}^\dagger(\mathbf{r}', t')]_{\pm} \rangle. \quad (2.13)$$

Using the previous definitions, one can find the relations between Retarded, Advanced, Greater and Lesser functions

$$G^R(\mathbf{r}, t, \mathbf{r}', t') = \theta(t - t') (G^>(\mathbf{r}, t, \mathbf{r}', t') - G^<(\mathbf{r}, t, \mathbf{r}', t')), \quad (2.14)$$

$$G^A(\mathbf{r}, t, \mathbf{r}', t') = \theta(t' - t) (G^<(\mathbf{r}, t, \mathbf{r}', t') - G^>(\mathbf{r}, t, \mathbf{r}', t')), \quad (2.15)$$

$$G^R(\mathbf{r}, t, \mathbf{r}', t') - G^A(\mathbf{r}, t, \mathbf{r}', t') = G^>(\mathbf{r}, t, \mathbf{r}', t') - G^<(\mathbf{r}, t, \mathbf{r}', t'). \quad (2.16)$$

Finally, we define a key function to the study of non-equilibrium systems, the so-called Kinetic or Keldysh Green's function

$$G^K(\mathbf{r}, t, \mathbf{r}', t') = G^>(\mathbf{r}, t, \mathbf{r}', t') + G^<(\mathbf{r}, t, \mathbf{r}', t'). \quad (2.17)$$

The G^K function, as we shall see, is strictly related to the distribution function appearing in the BTE, thus, it will be used many times.

2.4. More on Green's functions

One usually first hear about Green's functions as a method to solve ordinary and partial differential equations, for instance, in physics it can be used to find the electric potential (MACHADO, 2007). We've seen so far another amazing meaning and wrote relations that we haven't put to use yet, however, in this section we finally use it to solve a differential equation, the Schrödinger equation. The result extracted is fascinating, known as *Dyson equation*, the statistical nature of Green's functions will appear naturally.

Consider the Schrödinger equation (and omitting the spin dependency)

$$(i\partial_t - H(\mathbf{r}))\Psi(\mathbf{r}, t) = 0, \quad (2.18)$$

with

$$H = H_0(\mathbf{r}) + V(\mathbf{r}), \quad (2.19)$$

H_0 is the free part of the Hamiltonian and $V(\mathbf{r})$ is a perturbation. To solve this differential equation, it is interesting to introduce the Green's functions as

$$[i\partial_t - H_0(\mathbf{r})]G_0(\mathbf{r}, t, \mathbf{r}', t') = \delta(\mathbf{r} - \mathbf{r}')\delta(t - t'), \quad (2.20)$$

$$[i\partial_t - H_0(\mathbf{r}) - V(\mathbf{r})]G(\mathbf{r}, t, \mathbf{r}', t') = \delta(\mathbf{r} - \mathbf{r}')\delta(t - t'). \quad (2.21)$$

We also define the identities

$$G_0^{-1}(\mathbf{r}, t, \mathbf{r}', t') = (i\partial_t - H_0(\mathbf{r}))\delta(\mathbf{r} - \mathbf{r}')\delta(t - t'), \quad (2.22)$$

$$G^{-1}(\mathbf{r}, t, \mathbf{r}', t') = (i\partial_t - H_0(\mathbf{r}) - V(\mathbf{r}))\delta(\mathbf{r} - \mathbf{r}')\delta(t - t'), \quad (2.23)$$

$$G_0^{-1}(\mathbf{r}, t, \mathbf{r}', t', E)G_0(\mathbf{r}, t, \mathbf{r}', t') = \delta(\mathbf{r} - \mathbf{r}')\delta(t - t'), \quad (2.24)$$

$$G^{-1}(\mathbf{r}, t, \mathbf{r}', t', E)G(\mathbf{r}, t, \mathbf{r}', t') = \delta(\mathbf{r} - \mathbf{r}')\delta(t - t'). \quad (2.25)$$

To prove these identities note that Green's functions have matrix structures*, for instance

$$G_0(\mathbf{r}, \mathbf{r}') = \left[\begin{array}{ccc} \dots & \dots & \dots \\ \dots & G_0(\mathbf{r}, \mathbf{r}') & \dots \\ \vdots & \vdots & \ddots \end{array} \right]_{\mathbf{r}, \mathbf{r}'}, \quad (2.26)$$

where are the \mathbf{r} lines and \mathbf{r}' columns. Consider the matrix G_0 and its inverse G_0^{-1} , by definition

$$\sum_{\mathbf{r}''} G_0^{-1}(\mathbf{r}, \mathbf{r}'', E)G_0(\mathbf{r}'', \mathbf{r}', E) = \delta(\mathbf{r} - \mathbf{r}'), \quad (2.27)$$

*Ignoring the time dependency

the sum becomes an integral,

$$\int dr'' G_0^{-1}(\mathbf{r}, \mathbf{r}'') G_0(\mathbf{r}'', \mathbf{r}') = \delta(\mathbf{r} - \mathbf{r}') \quad (2.28)$$

and replacing Eq. 2.22 in the equation above

$$\int dr'' (i\partial_t - H_0(\mathbf{r})) \delta(\mathbf{r} - \mathbf{r}'') G_0(\mathbf{r}'', \mathbf{r}') = \delta_{r, r'}, \quad (2.29)$$

we recover the Green's functions definition for the Schrödinger equation

$$[i\partial_t - H_0(\mathbf{r})] G_0(\mathbf{r}, \mathbf{r}') = \delta(\mathbf{r} - \mathbf{r}'). \quad (2.30)$$

With Eqs. 2.22 and 2.24 the Schrödinger equation is written

$$G_0^{-1}(\mathbf{r}, t) \Psi(\mathbf{r}, t) = V(\mathbf{r}) \Psi(\mathbf{r}, t), \quad (2.31)$$

and for a free system

$$G_0^{-1}(\mathbf{r}, t) \Psi_0(\mathbf{r}, t) = 0, \quad (2.32)$$

subtracting** 2.31 by 2.32

$$G_0^{-1}(\mathbf{r}, t) (\Psi(\mathbf{r}, t) - \Psi_0(\mathbf{r}, t)) = V(\mathbf{r}) \Psi(\mathbf{r}, t), \quad (2.33)$$

multiplying by $G(\mathbf{r}, t, \mathbf{r}', t')$ and integrating

$$\begin{aligned} \int dt' \int d\mathbf{r}' G_0^{-1}(\mathbf{r}, t) G_0(\mathbf{r}, t, \mathbf{r}', t') (\Psi(\mathbf{r}', t') - \Psi_0(\mathbf{r}', t')) &= \int dt' \int d\mathbf{r}' G_0(\mathbf{r}, t) V(\mathbf{r}) \Psi(\mathbf{r}', t') \\ \Psi(\mathbf{r}, t) &= \Psi_0(\mathbf{r}, t) + \int dt' \int d\mathbf{r}' G_0(\mathbf{r}, t, \mathbf{r}', t') V(\mathbf{r}) \Psi(\mathbf{r}', t') \end{aligned} \quad (2.34)$$

iterating the solution*,

$$\begin{aligned} \Psi &= \Psi_0 + G_0 V \Psi_0 + G_0 V G_0 V \Psi_0 + G_0 V G_0 V G_0 V \Psi_0 + \dots \\ &= \Psi_0 + (G_0 + G_0 V G_0 + G_0 V G_0 V G_0 + \dots) V \Psi_0. \end{aligned} \quad (2.35)$$

Using the relation $G^{-1} = G_0^{-1} - V$ and following the same steps to get Eq. 2.34, one can also encounter a result for the full Green Function G

$$\begin{aligned} \int dt' \int d\mathbf{r}' G^{-1}(\mathbf{r}, t) G(\mathbf{r}, t) (\Psi(\mathbf{r}', t') - \Psi_0(\mathbf{r}', t')) &= \int dt' \int d\mathbf{r}' G_0(\mathbf{r}, t) V(\mathbf{r}) \Psi_0(\mathbf{r}', t'), \\ \Psi(\mathbf{r}, t) &= \Psi_0(\mathbf{r}, t) + \int dt' \int d\mathbf{r}' G(\mathbf{r}, t) V(\mathbf{r}) \Psi_0(\mathbf{r}', t'). \end{aligned} \quad (2.36)$$

Comparing Eqs. 2.36 and 2.35 one note

$$G = G_0 + G_0 V (G_0 + G_0 V G_0 + \dots), \quad (2.37)$$

**Notice that if one had summed the two equations we would have gotten a different result, the reason a sum is not allowed, is that if $V(\mathbf{r})$ were to be zero, the result would be Ψ_0 with a minus sign.

*The integrals are often omitted or replaced by the symbol $\otimes = \int dt' \int d\mathbf{r}'$ and also we opt to omit the variables dependency (r, t) .

or, the famous result known as the Dyson equation

$$G = G_0 + G_0 V G. \quad (2.38)$$

Eq. 2.38 is also written in a very useful way

$$G = \frac{1}{G_0^{-1} - V}. \quad (2.39)$$

Solving the Schrödinger equation show us that just like quantum mechanics, Green's functions have a probabilistic nature, and its statistical essence is represented by the Dyson equation. From Eq. 2.35 one notice that each individual term represents a way a particle can propagate from one point to another, for a physical intuition appeal, it is represented by the figure 2, an infinity series of possibilities, or, as we've seen for quantum propagators, infinity probability amplitudes.

From this point forward carrying all the variables[‡] dependencies could be tiresome, thus, we introduce a compact notation $(1, 1') = (\mathbf{r}, t, \mathbf{r}', t')$.

2.5. An introduction to Feynman Diagrams

In this section we introduce the use of Feynman diagrams in the quantum many body theory. Named after its inventor Richard Feynman, it is a pictorial way to describe complex interactions that would be way harder to grasp intuitively. "Feynman diagrams helped to transform the way physicists saw the world, and their place in it" (KAISER, 2005), is a powerful tool used in non-equilibrium problems, a whole field that deserves a special attention, although, we shall not get into much detail. The reader is highly recommended the reference (MATTUCK, 1992), where the author introduce the diagrams in a marvelous way. The purpose of this section is a pedagogical introduction into the diagrammatic expansion in many body quantum theory which give us an intuition of the non-equilibrium problem. We shall later on, use the actual diagrams for specific interactions. We'll start by again deducing, diagrammatically, Dyson's equation 2.38, first presented in the section 2.4.

We'll start with a dictionary of what each term of the equation mean*

$$G(1, 1') = \begin{array}{|c} \parallel \\ \parallel \\ \uparrow \end{array}, \quad G_0(1, 1') = \begin{array}{|c} | \\ \uparrow \\ | \end{array}, \quad V = \begin{array}{|c} \circ \\ \text{V} \\ \circ \end{array}, \quad (2.40)$$

[‡]even if we have omitted spin

*Note that these are not the actual Diagrams, V can be any type of interaction where we'll have a type o diagram for which one, the diagrams for G_0 and G are the representation for Fermions, we might as well have photon diagrams which are not arrows, but rather wiggling lines.

it's important to emphasize that the diagram for V is a generic one, hence, the well-known Dyson equation can be written diagrammatic as

$$G(1, 1') = \begin{array}{c} \parallel \\ \uparrow \end{array} = \begin{array}{c} | \\ \uparrow \end{array} + \begin{array}{c} \uparrow \\ \circ V \\ \uparrow \end{array} + \begin{array}{c} \uparrow \\ \circ V \\ \uparrow \\ \circ V \\ \uparrow \end{array} + \begin{array}{c} \uparrow \\ \circ V \\ \uparrow \\ \circ V \\ \uparrow \\ \circ V \\ \uparrow \end{array} + \dots \quad (2.41)$$

$$G(1, 1') = \begin{array}{c} \parallel \\ \uparrow \end{array} = \begin{array}{c} | \\ \uparrow \end{array} \left[1 + \begin{array}{c} \uparrow \\ \circ V \\ \uparrow \end{array} + \begin{array}{c} \uparrow \\ \circ V \\ \uparrow \\ \circ V \\ \uparrow \end{array} + \begin{array}{c} \uparrow \\ \circ V \\ \uparrow \\ \circ V \\ \uparrow \\ \circ V \\ \uparrow \end{array} + \dots \right] \quad (2.42)$$

$$\begin{array}{c} \parallel \\ \uparrow \end{array} = \begin{array}{c} | \\ \uparrow \end{array} \left[1 + \begin{array}{c} \uparrow \\ \circ V \\ \uparrow \end{array} + \left(\begin{array}{c} \uparrow \\ \circ V \\ \uparrow \end{array} \right)^2 + \left(\begin{array}{c} \uparrow \\ \circ V \\ \uparrow \end{array} \right)^3 + \dots \right] \quad (2.43)$$

Note that the diagrams behave like a series $\sum_{n=0}^{\infty} x^n = \frac{1}{1-x}$, therefore

$$G(1, 1') = \begin{array}{c} \parallel \\ \uparrow \end{array} = \begin{array}{c} | \\ \uparrow \end{array} \times \frac{1}{\left[1 - \begin{array}{c} \uparrow \\ \circ V \\ \uparrow \end{array} \right]} \quad (2.44)$$

$$\begin{array}{c} \parallel \\ \uparrow \end{array} = \frac{1}{\left[\begin{array}{c} | \\ \uparrow \end{array} \right]^{-1} - \begin{array}{c} \uparrow \\ \circ V \\ \uparrow \end{array}} \quad (2.45)$$

and 2.39 is recovered, but in the diagrammatic form.

2.6. Self-Energy

Writing Dyson's equation in a diagrammatic form is an incredible easier approach to deduce important information. In the last section we were considering only one kind of

interaction, V , in this section we shall consider another kind of interaction X . For two or higher types of interactions we use the so-called *self-energy* Σ .

Before employing the interaction X in the Dyson equation, we have to note a very important point about the self-energy and its definition. There are two kind of diagrams, *reducible* and *irreducible* (MATTUCK, 1992), their difference is, reducible ones can be broken into irreducible. The self-energy is the sum of all irreducible diagrams. We shall not depicted the their difference, for simplicity \textcircled{V} and \textcircled{X} are irreducible ones. Once define the so-called self-energy, we shall see that it will appear naturally in the diagrammatic form. The Dyson equation for two kinds of interaction V and X is

$$\begin{aligned}
 & \parallel \uparrow = \uparrow + \textcircled{V} + \textcircled{X} + \begin{array}{c} \uparrow \\ \textcircled{V} \\ \uparrow \end{array} + \begin{array}{c} \uparrow \\ \textcircled{X} \\ \uparrow \end{array} + \dots \\
 & + \begin{array}{c} \uparrow \\ \textcircled{V} \\ \uparrow \\ \textcircled{X} \\ \uparrow \end{array} + \begin{array}{c} \uparrow \\ \textcircled{X} \\ \uparrow \\ \textcircled{V} \\ \uparrow \end{array} + \begin{array}{c} \uparrow \\ \textcircled{V} \\ \uparrow \\ \textcircled{V} \\ \uparrow \\ \textcircled{V} \\ \uparrow \end{array} + \begin{array}{c} \uparrow \\ \textcircled{X} \\ \uparrow \\ \textcircled{X} \\ \uparrow \\ \textcircled{X} \\ \uparrow \end{array} + \begin{array}{c} \uparrow \\ \textcircled{X} \\ \uparrow \\ \textcircled{V} \\ \uparrow \\ \textcircled{V} \\ \uparrow \end{array} + \begin{array}{c} \uparrow \\ \textcircled{V} \\ \uparrow \\ \textcircled{X} \\ \uparrow \\ \textcircled{X} \\ \uparrow \end{array} + \dots, \quad (2.46)
 \end{aligned}$$

the diagrams above can be broken into

$$\begin{aligned}
 & \parallel \uparrow = \uparrow \times \left[1 + \uparrow \times \textcircled{V} + \uparrow \times \textcircled{X} + \begin{array}{c} \uparrow^2 \\ \times \textcircled{V}^2 \end{array} + \begin{array}{c} \uparrow^2 \\ \times \textcircled{X}^2 \end{array} \right. \\
 & + 2 \times \begin{array}{c} \uparrow^2 \\ \times \textcircled{X} \times \textcircled{V} \end{array} + \begin{array}{c} \uparrow^3 \\ \times \textcircled{V}^3 \end{array} + \begin{array}{c} \uparrow^3 \\ \times \textcircled{X}^3 \end{array} + \begin{array}{c} \uparrow^3 \\ \times \textcircled{X}^2 \times \textcircled{V} \end{array} \\
 & \left. + \begin{array}{c} \uparrow^3 \\ \times \textcircled{V}^2 \times \textcircled{X} \end{array} + \dots \right], \quad (2.47)
 \end{aligned}$$

patterns start to emerge and are put in evidence

$$\parallel \uparrow = \uparrow \times \left[1 + \uparrow \times \left(\textcircled{V} + \textcircled{X} \right) + \begin{array}{c} \uparrow^2 \\ \times \left(\textcircled{V} + \textcircled{X} \right)^2 \end{array} + \dots \right],$$

as in Eq. 2.43,

$$\begin{array}{c} \parallel \\ \uparrow \end{array} = \frac{1}{\left[\begin{array}{c} \uparrow \\ \uparrow \\ - \left(\textcircled{V} + \textcircled{X} \right) \end{array} \right]^{-1}}, \tag{2.48}$$

by the definition of self-energy, the Dyson equation now is written as

$$\begin{array}{c} \parallel \\ \uparrow \end{array} = \frac{1}{\left[\begin{array}{c} \uparrow \\ \uparrow \\ - \textcircled{\Sigma} \end{array} \right]^{-1}} \tag{2.49}$$

or mathematically,

$$G = \frac{1}{G_0^{-1} - \Sigma} \tag{2.50}$$

The self-energy is also a infinity series of diagrams for the case of infinity interactions

$$\textcircled{\Sigma} = \textcircled{V} + \textcircled{X} + \dots \tag{2.51}$$

A more general Dyson equation can be written diagrammatically

$$G(1, 1') = \begin{array}{c} \parallel \\ \uparrow \end{array} = \begin{array}{c} \uparrow \\ \uparrow \end{array} + \begin{array}{c} \uparrow \\ \textcircled{\Sigma} \\ \uparrow \end{array} + \begin{array}{c} \uparrow \\ \textcircled{\Sigma} \\ \uparrow \\ \textcircled{\Sigma} \\ \uparrow \end{array} + \begin{array}{c} \uparrow \\ \textcircled{\Sigma} \\ \uparrow \\ \textcircled{\Sigma} \\ \uparrow \\ \textcircled{\Sigma} \\ \uparrow \end{array} + \dots \tag{2.52}$$

or mathematically

$$G = G_0 + G_0 \Sigma G. \tag{2.53}$$

It's amazing how physicists can simplify a problem to be workable with. The self-energy do this job, it simplifies all the unknown interactions into one thing. Writing it as a series within the Dyson equation, we will see that it also has a matrix form.

Dealing with non-equilibrium physics one has to deal with concepts and mathematical tools that are hard to grasp. Therefore, the last two sections were meant as introduction to Feynman diagrams, writing generic diagrams and seeing how they behave in the Dyson equations diagrammatically, is an attempt to give a new reader an intuitively way to deal with non-equilibrium problems.

2.7. Time evolution operators and the closed path formalism

In this section we introduce the closed path formalism. To work with a system in equilibrium some tricks and mathematical tools are enough, however, when it comes to non-equilibrium a further step have to be taken. The closed path formalism is based in the equivalency of the time evolution operators between the Heisenberg and Interaction pictures. In order to avoid confusion of which representation we are working with, the states and operators are labeled with the subscripts

- \mathcal{H} – Heisenberg picture
- I – Interaction picture
- S – Schrödinger picture

In the non-equilibrium problem we mainly deal with the Hamiltonian

$$\mathcal{H} = H_0 + V(t), \quad (2.54)$$

where H_0 is the free Hamiltonian and $V(t)$ the time-dependent perturbation.

Table 1 is a summary of the state vectors and operators of the three pictures

	Schrödinger picture	Heisenberg picture	Interaction picture
States Vectors	$ \Psi_S(t)\rangle = U_{\mathcal{H}}(t, t_0) \Psi_S(t_0)\rangle$	States are time-independent	$ \Psi_I(t)\rangle = U_I(t, t_0) \Psi_I(t_0)\rangle$
Time evolution operators	$U_{\mathcal{H}}(t, t_0) = e^{-iH(t-t_0)}$	$U_{\mathcal{H}}(t, t_0) = e^{-iH(t-t_0)}$	$U_I(t, t_0) = e^{-i \int_{t_0}^t V_I(t') dt'}$
Operators	\hat{O}_S	$\hat{O}_{\mathcal{H}}(t)$	$\hat{O}_I(t)$

Table 1 – Time evolution operators in each representation of quantum mechanics

Next we deduce the relation between the time evolution operators in the Heisenberg and Interaction pictures, that are the foundation in which the closed path formalism is based. We start by the relation between the state vector in the Schrödinger and Interaction pictures are related by

$$|\Psi_S(t)\rangle \equiv U_{H_0}(t, t_0) |\Psi_I(t)\rangle, \quad (2.55)$$

where $U_{H_0} = e^{-iH_0(t-t_0)}$. Using table 1 and Eq. 2.55

$$U_{\mathcal{H}}(t, t_0) |\Psi_S(t_0)\rangle = U_{H_0}(t, t_0) U_I(t, t_0) |\Psi_I(t_0)\rangle. \quad (2.56)$$

Consider t_0 as the time where all the pictures coincide, therefore

$$U_{\mathcal{H}}(t, t_0) = U_{H_0}(t, t_0) U_I(t, t_0), \quad (2.57)$$

$$U_I(t, t_0) = U_{\mathcal{H}}(t, t_0) U_{H_0}^\dagger(t, t_0). \quad (2.58)$$

Heisenberg picture	Interaction picture
$\hat{O}_{\mathcal{H}}(t) = U_{\mathcal{H}}^{\dagger}(t, t_0) \hat{O}_S U_{\mathcal{H}}(t, t_0)$	$\hat{O}_I(t) = U_{H_0}^{\dagger}(t, t_0) \hat{O}_S U_{H_0}(t, t_0)$

Table 2 – Relation between operator in Heisenberg’s and interaction pictures with an operator in Schöndiger’s picture

When working with Green’s functions the field operators are in the Heisenberg picture, therefore, the main goal here is to shift it to the Interaction picture. Table 2 displays general operators in both pictures using time evolution operators

Using $U(t, t'')U(t'', t') = U(t, t')$ one relates the operators by associating the equations from table 2

$$\hat{O}_{\mathcal{H}}(t) = U_{\mathcal{H}}^{\dagger}(t, t_0)U_{H_0}(t, t_0)\hat{O}_I(t)U_{H_0}^{\dagger}(t, t_0)U_{\mathcal{H}}(t, t_0), \quad (2.59)$$

and from Eq.(2.58)

$$\hat{O}_{\mathcal{H}}(t) = U_I^{\dagger}(t, t_0)\hat{O}_I(t)U_I(t, t_0). \quad (2.60)$$

Equation 2.60 is an important relation to guide us through the transition between real time to closed time path formalism. Now the field operators in Green’s functions can be written in the Interaction picture.

We wish to study non-equilibrium phenomena, consider an arbitrary physical system described by the Hamiltonian

$$\mathcal{H} = H_0 + V(t). \quad (2.61)$$

To this end, we introduce the so-called closed path formalism, which consists of a contour c , enclosing the real time axis as depicted in Fig. (3). Each point on the contour correspond to a point in the real time axis. From a time evolution point of view, it starts in t_0 , goes all the way to t , and then back again to t_0 .

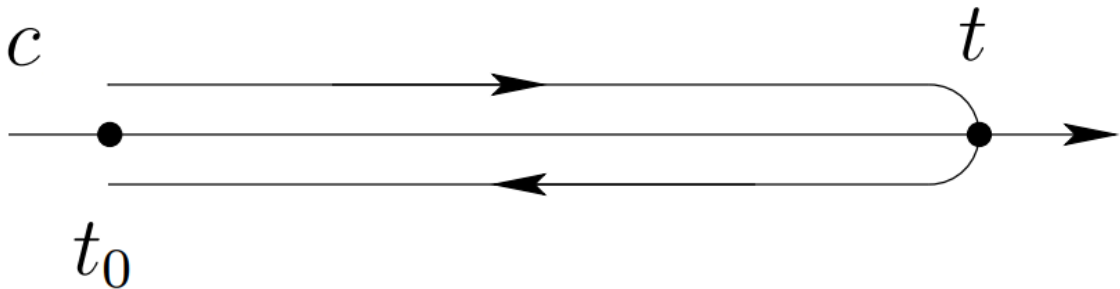


Figure 3 – Close time path c [extracted from Ref. (RAMMER, 2007)].

One goes from real time to contour variables using the connection between operators in the Heisenberg and interaction pictures, as shown in Appendix (B). The transformation between the two pictures can be expressed as

$$\hat{O}_{\mathcal{H}}(t) = T_c \left(e^{-i \int_c d\tau V_I(\tau)} \hat{O}_I(t) \right), \quad (2.62)$$

with τ as the contour variable, which is equivalent to Eq. (2.60). Here, the indexes \mathcal{H} and I represents the operators in the Heisenberg and interaction pictures, respectively. The contour ordering operator T_c display the same features as the normal time ordering operator, it orders the products of operators according to the position of their respective contour variables in the contour c , later variables are placed to the right. For instance, a pair of generic operators \hat{A} and \hat{B} , one has

$$T_c \left(\hat{A}(\tau) \hat{B}(\tau') \right) = \begin{cases} \hat{A}(\tau) \hat{B}(\tau'), & \tau > \tau', \\ \mp \hat{B}(\tau') \hat{A}(\tau), & \tau' > \tau, \end{cases} \quad (2.63)$$

where the $-$ and $+$ signs are for fermions and bosons, respectively. Notice that, here, the comparison $\tau > \tau'$ states that τ occurs later in the contour of Fig. (3).

2.8. Green's Function in the Closed Path formalism

The central goal of non-equilibrium theory is to compute the average of real-time correlation functions. That is, we wish to calculate

$$G(\mathbf{r}, t, \mathbf{r}', t) = -i \left\langle T \psi_{\mathcal{H}}(\mathbf{r}, t) \psi_{\mathcal{H}}^{\dagger}(\mathbf{r}', t') \right\rangle = \text{tr} \left(\rho T \psi_{\mathcal{H}}(\mathbf{r}, t) \psi_{\mathcal{H}}^{\dagger}(\mathbf{r}', t') \right). \quad (2.64)$$

Provided the closed path formalism, we write Eq. (2.64) on it's framework. Note the time dependence variables t_1 and t'_1 , there must be two contour variables linked to it, in fact, as depicted in figure (4).

Green's functions may depend upon many variables (position, time, spin, etc.). One can get lost carrying all these variables, turning some calculations into a tough job. Therefore, as for contour variables, we use the compact notation, $(\mathbf{r}_1, \tau_1) = 1$ and $(\mathbf{r}'_1, \tau'_1) = 1'$.

$$G(1, 1') = -i \frac{\text{tr} \left(\rho^{-\beta H} T_c \left(\psi_{\mathcal{H}}(1) \psi_{\mathcal{H}}^{\dagger}(1') \right) \right)}{\text{tr} \left(e^{-H\beta} \right)} = -i \left\langle T_c \psi_{\mathcal{H}}(1) \psi_{\mathcal{H}}^{\dagger}(1') \right\rangle, \quad (2.65)$$

where,

$$G(1, 1') = \begin{cases} G^{<}(1, 1') & \tau_{1'} > \tau_1 \\ G^{>}(1, 1') & \tau_1 > \tau_{1'}. \end{cases} \quad (2.66)$$

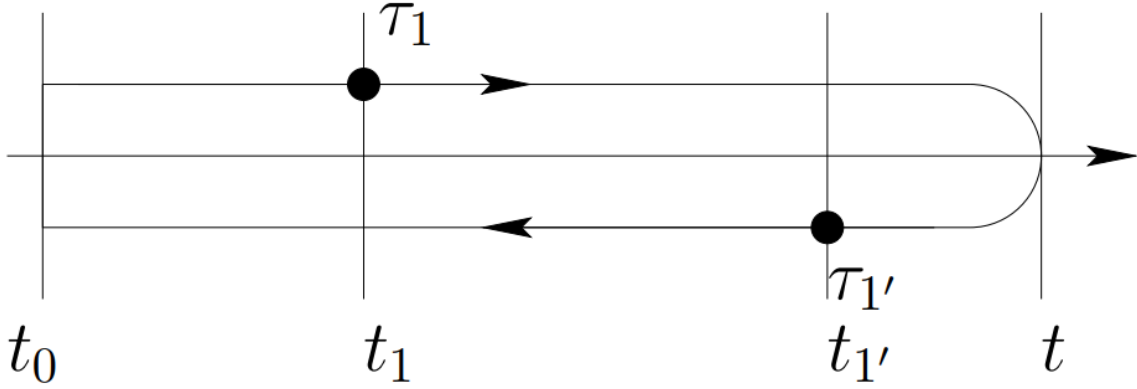


Figure 4 – Time variables of the Green's function and their respective contour variables [extracted from Ref. (RAMMER, 2007)].

The field operators are still in the Heisenberg picture. According to Eq. (2.62) the Green function in the interaction picture is

$$G(1, 1') = -i \left\langle T_{c_1} \left(e^{-i \int_{c_1} d\tau V_I(\tau)} \psi_I(1) \right) T_{c_{1'}} \left(e^{-i \int_{c_{1'}} d\tau V_I(\tau)} \psi_I^\dagger(1') \right) \right\rangle. \quad (2.67)$$

One can add the two contours, yielding a total contour $c = c_{1'} + c_1$. You must be wondering, why can we sum two contours? The integral part in (2.62) is equivalent to a time evolution operator (see appendix (B)). To give a perspective of what summing two contours mean, we recall the equivalency of Eqs. (2.60) and (2.62) and go back to real time, thus, Eq. (2.67) is reciprocal to

$$\begin{aligned} G(1, 1') &= -i \left\langle T_{c_1} \left(U_I^\dagger(1, t_0) \psi_I(1) U_I(1, t_0) \right) T_{c_{1'}} \left(U_I(t_0, 1) \psi_I^\dagger(1') U_I^\dagger(t_0, 1') \right) \right\rangle \\ &= -i \left\langle T_{c_1+c_{1'}} \left(U_I^\dagger(1, t_0) \psi_I(1) U_I(1, t_0) U(t_0, 1') \psi_I^\dagger(1') U_I^\dagger(t_0, 1') \right) \right\rangle \\ &= -i \left\langle T_{c_1+c_{1'}} \left(U_I^\dagger(1, t_0) \psi_I(1) U_I(1, 1') \psi_I^\dagger(1') U_I^\dagger(t_0, 1') \right) \right\rangle. \end{aligned} \quad (2.68)$$

Dealing with non-equilibrium, one will often come across time evolution operators like $U_I(1, 1')^*$ in the last equality. The trick is to consider $t = \text{Max}[t_1, t_{1'}]$, which means the maximum value of the respective time evolution, corresponding the maximum values of c_1 and $c_{1'}$. Therefore, $U_I(1, 1') = U(t, t) = 1$, “blending” the contours together, as depicted in figure 5**, forming a contour c as in figure 3. The Eq. (2.68) becomes

$$G(1, 1') = -i \left\langle T_c \left(U_I^\dagger(t, t_0) \psi_I(1) \psi_I^\dagger(1') U_I^\dagger(t_0, t) \right) \right\rangle, \quad (2.69)$$

or equivalent ,

*Since we're dealing with time evolution operator $1 = t_1$ and $1' = t_{1'}$.

**The figure suggests $t_{1'} > t_1$, but is not necessarily true, since it could be the other way around

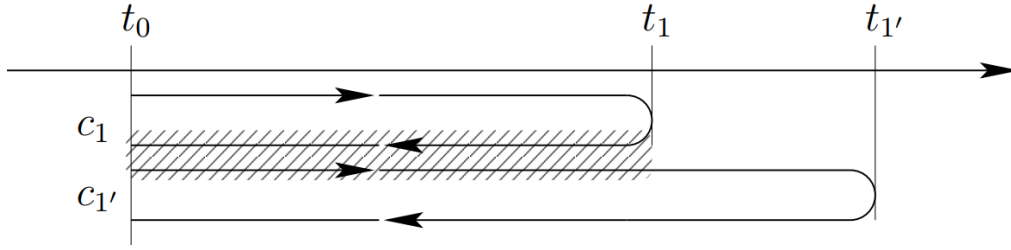


Figure 5 – Summing the contour c_1 and $c_{1'}$, the shaded region cancels and we recover the contour c depicted (3) with $t = \max(t_1, t_{1'})$

$$\begin{aligned}
 G(1, 1') &= -i \left\langle T_{c_1+c_{1'}} \left(e^{-i \int_{c_1+c_{1'}} d\tau V_I(\tau)} \psi_I(1) \psi_I^\dagger(1') \right) \right\rangle \\
 &= -i \left\langle T_c \left(e^{-i \int_c d\tau V_I(\tau)} \psi_I(1) \psi_I^\dagger(1') \right) \right\rangle.
 \end{aligned} \tag{2.70}$$

To summarize, we can add the contours on the grounds that is equivalent to use the properties of the time evolution operators. One can also ask, why shouldn't we just work with the time evolution operator then? The reason is that in non-equilibrium systems we are interested in asymptotic past and future, that means leaving the time evolution operators with times in the infinity. It's hard to work with such operators. Eq. (2.70) is almost the final form to gain information about the system, in the next sections we'll proceed with new mathematical tools which enable us to go further into the non-equilibrium problem.

2.9. The Keldysh Formalism

In this section we introduce the Keldysh formalism. It consists of a two branch contour that creates the Schwinger-Keldysh Space. We shall see why such contour allow a much easier way to deal with non-equilibrium problems. On the other hand, to get there, we have compute the average of Eq. (2.70), viz.

$$G(1, 1') = -i \frac{\text{tr} \left(e^{-\beta \mathcal{H}} T_c \left[e^{-i \int_c d\tau V_I(\tau)} \psi_I(1) \psi_I^\dagger(1') \right] \right)}{\text{tr} \left(e^{-\beta \mathcal{H}} \right)}, \tag{2.71}$$

a job that's not easily done.

One realize that expanding the integral in Eq. (2.71) an infinity string of field operators will appear, in other words, an infinity summation of them.

There's a method from quantum field theory, called Wick's theorem(see appendix (C)), which enable one to break down the string of operators into pairs. However, to employ it, we need to set the Eq. (2.71) to some conditions. First, the field operators ψ_I and ψ_I^\dagger

are required to evolve with a non-interacting Hamiltonian (MACIEJKO, 2007) (which they already are, since we manage to write them in the Interaction picture). Second,

$$e^{-\beta\mathcal{H}} = e^{-\beta H_0} T_{c_a} e^{-i \int_{t_0}^{t_0-i\beta} d\tau V_I(\tau)}, \quad (2.72)$$

we need a non-interacting density matrix in the Boltzmann weighting factor[§] (DANIELEWICZ, 1984).

One needs to “fit” Eq. (2.71) under these conditions in order to Wick’s theorem be applied. One way to do it, is by adding a complex appendix to the contour in figure 3, where the complex limit $t_0 - i\beta$ is introduced as depicted in figure 6. This is also known as the Kadanoff-Baym contour (RAMMER, 2007). Considering the new complex contour,

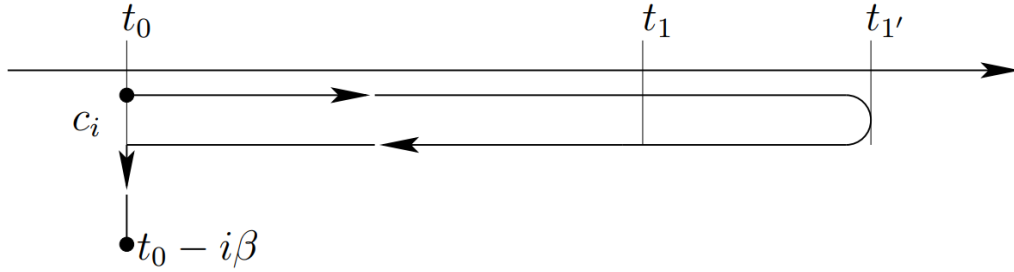


Figure 6 – complex appendix added so that one can obtain the free density matrix (extracted from Ref (RAMMER, 2007)).

the Green function becomes

$$G(1, 1') = -i \frac{\text{tr} \left[e^{-\beta H_0} \left(T_{c_a} e^{-i \int_{t_0}^{t_0-i\beta} V_I(t) dt} \right) T_c \left(e^{-i \int_c d\tau V_I(\tau)} \psi_I(1) \psi_I^\dagger(1') \right) \right]}{\text{tr} \left(e^{-\beta H_0} T_{c_a} e^{-i \int_{t_0}^{t_0-i\beta} V_I(t) dt} \right)}. \quad (2.73)$$

We’ve seen that the contours can be added together, due to their time evolution properties, in this case we create the contour c_i by adding c and c_a . Multiplying the numerator and denominator by $T_c e^{-i \int_{t_0}^{t_0-i\beta} V_I(t) dt}$ yields c_i , enabling one to write

$$G(1, 1') = -i \frac{\text{tr} \left(e^{-\beta H_0} T_{c_i} \left[e^{-i \int_{c_i} d\tau V_I(\tau)} \psi_I(1) \psi_I^\dagger(1') \right] \right)}{\text{tr} \left(e^{-\beta H_0} T_{c_i} e^{-i \int_{c_i} V_I(t) dt} \right)}. \quad (2.74)$$

We must be careful handling the equation above, it looks complicated, so we still need to simplify it for a suitable use of Wick’s theorem. A close look at the denominator show that is essentially the time evolution forward and backward in a contour[¶], namely

[§]The details of this derivation can be seen in appendix A

[¶]Note that $T_{c_i} e^{-i \int_{c_i} V_I(t) dt}$ is not followed by any field operator, thus, this argument is cannot be used for the numerator

from t_0 to $\max[t_1, t_{1'}]$ and back again. Mathematically speaking

$$U(\text{inicial time of the contour}, \max[t_1, t_{1'}])U(\max[t_1, t_{1'}], \text{inicial time of the contour}) = 1. \quad (2.75)$$

The contour ordered term in the denominator is one, remaining solely the partition $\text{tr}(e^{-\beta H_0})$ function

$$G(1, 1') = -i \text{tr} \left(\rho_0 T_{c_i} \left[e^{-i \int_{c_i} d\tau V_I(\tau)} \psi_I(1) \psi_I^\dagger(1') \right] \right), \quad (2.76)$$

where,

$$\rho_0 = \frac{e^{-\beta H_0}}{\text{tr}(e^{-\beta H_0})}. \quad (2.77)$$

Appreciate the result for a second, we manage to write the Green function for a general non-equilibrium system using the statistical operator for the equilibrium case, which is easier to deal with. Hence the power of the method.

We will take a step further and do not consider initial correlations, i.e., we do not consider how the system was prior to t_0 and let it approach to minus infinity. It has been shown (RAMMER, 2007) that ignoring initial correlations amount to neglect the complex appendix. Therefore, we have the so-called Keldysh contour depicted in figure 7 and denoting the forward \vec{c}_1 and the backward part \overleftarrow{c}_2 .

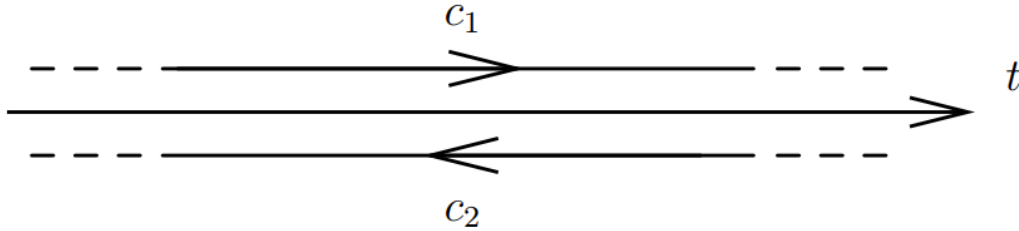


Figure 7 – Keldysh contour [extracted from Ref. (RAMMER, 2007)].

2.10. Using Wick's theorem

From last chapter we've obtained a general non-equilibrium Green's function and now it's time to put it to use. We start by the simplest kind of coupling, that is, particles coupled to external field $V(\mathbf{r}, \tau)$ (KADANOFF, 2018), hence, the interaction part of the Hamiltonian becomes $V_I(\tau) = V(\mathbf{r}, \tau) \psi_I^\dagger(\mathbf{r}, \tau) \psi_I(\mathbf{r}, \tau)$, which leads equation (2.75) to

$$G(1, 1') = \text{tr} \left(\rho_0 T_c \left(e^{-i \int_c d\mathbf{r} V(\mathbf{r}, \tau) \psi_I^\dagger(\mathbf{r}, \tau) \psi_I(\mathbf{r}, \tau)} \psi_I(1) \psi_I^\dagger(1') \right) \right). \quad (2.78)$$

Expanding, the zeroth-order yields the free Green's function

$$G^0(1, 1') = -i \text{tr} \left(\rho_0 T_c \left(\psi_I^\dagger(1) \psi_I(1') \right) \right). \quad (2.79)$$

For the first order,

$$G^1(1, 1') = (-i)^2 \int d\mathbf{r}_2 \int_c d\tau_2 V(2) \text{tr} \left(\rho_0 T_c \left(\psi_I^\dagger(2) \psi_I(2) \psi_I(1) \psi_I^\dagger(1') \right) \right). \quad (2.80)$$

If one continues to expand, a infinity string of field operators would appear. Since we're interested in the non-equilibrium situation we ought deal with the first-order expanded Green's function, because the zeroth-order doesn't take into account the perturbation and orders higher than two are quite complicated to work with. How to handle such equation? All the effort in writing the Green's function with the free density matrix, now pays off. We can expand further equation (2.80) using Wick's theorem in Appendix (C). Let's handle only the parts with the string of fermion fields

$$\begin{aligned} \text{tr} \left(\rho_0 T_c \left(\psi_I^\dagger(2) \psi_I(2) \psi_I(1) \psi_I^\dagger(1') \right) \right) &= \underbrace{\langle \psi_I^\dagger(2) \psi_I(2) \rangle}_{G^0(2,2)} \underbrace{\langle \psi_I(1) \psi_I^\dagger(1') \rangle}_{G^0(1,1')} + \\ &\quad \underbrace{\langle \psi_I^\dagger(2) \psi_I(1) \rangle}_{G^0(1,2)} \underbrace{\langle \psi_I(2) \psi_I^\dagger(1') \rangle}_{G^0(2,1')} + \\ &\quad \underbrace{\langle \psi_I^\dagger(2) \psi_I^\dagger(1') \rangle}_{0} \underbrace{\langle \psi_I(2) \psi_I(1) \rangle}_{0} \end{aligned} \quad (2.81)$$

The first term carries the equivalent $G^0(2, 2)$ function, it means we are destroying and creating a particle in the same position at the same time, it doesn't appeal as propagation physical sense, besides, by replacing in Eq.(2.80) one notice that integral is zero. The third term, from Appendix C, is trivially zero, leaving only the second term alive. Therefore, the Green's function becomes

$$G^1(1, 1') = \int d\mathbf{r}_2 \int_c d\tau_2 G^0(1, 2) V(2) G^0(2, 1'). \quad (2.82)$$

2.11. Schwinger-Keldysh Space

Everything we have been doing so far had the goal to get to this crucial point, the point where we construct the Keldysh Space. We introduced the closed path formalism and rewrite all operators within this formalism so we could build the Keldysh contour (figure 7) and then expand the correlation function using Wick's theorem. Next we construct what is known as the Schwinger-Keldysh space, provided by the Keldysh contour. It's helpful because within its framework, we work with one goal, find an easier and doable way to manipulate the correlation functions, and that's exactly what the Keldysh space provides.

Take a close look at the time dependency of the Green's Function $G(\mathbf{r}, t, \mathbf{r}', t') = G(1, 1')$ and recall we divided the contour in figure 7 into forward \vec{c}_1 and backward \overleftarrow{c}_2 parts. The variables in 1 and 1', can either be in the forward or backward parts at the same time or be in different parts.

In the Keldysh space $G(1, 1')$ becomes $\hat{G}_{ij}(1, 1')$ where the subscripts i and j represents the forward and backward contour respectively. Hence the matrix representation

$$\hat{G}(1, 1') \equiv \begin{bmatrix} \hat{G}_{11}(1, 1') & \hat{G}_{12}(1, 1') \\ \hat{G}_{21}(1, 1') & \hat{G}_{22}(1, 1') \end{bmatrix}, \quad (2.83)$$

the indexes represents whether the variable lie on forward part or backward part, labeled by 1 and 2 respectively. We analyze each component separately, for instance, the $\hat{G}_{11}(1, 1')$ component, both variables are in the forward contour and we have the causal Green's function

$$\hat{G}_{11}(1, 1') = G(1, 1') = -i \langle T(\psi(1)\psi^\dagger(1')) \rangle. \quad (2.84)$$

The $\hat{G}_{22}(1, 1')$ component, both variables are also in the same branch, however, in the backward part, that means a propagation backwards in time, hence is correspondent to

$$\hat{G}_{22}(1, 1') = \tilde{G}(1, 1') = -i \langle \tilde{T}(\psi(1)\psi^\dagger(1')) \rangle, \quad (2.85)$$

the anti-time-ordered Green Function. The $\hat{G}_{12}(1, 1')$ and $\hat{G}_{21}(1, 1')$ components are trickier because their variables aren't in the same branch of the contour. So we recall Eq. (2.7) and consider a variable in the forward contour greater than a variable in backward contour. Therefore,

$$\hat{G}_{12}(1, 1') = G^<(1, 1') = \mp i \langle (\psi^\dagger(1')\psi(1)) \rangle, \quad (2.86)$$

and

$$\hat{G}_{21}(1, 1') = G^>(1, 1') = i \langle (\psi(1)\psi^\dagger(1')) \rangle. \quad (2.87)$$

Finally we encounter the matrix

$$\hat{G}(1, 1') = \begin{bmatrix} G(1, 1') & G^<(1, 1') \\ G^>(1, 1') & \tilde{G}(1, 1') \end{bmatrix}, \quad (2.88)$$

The components of $\hat{G}(1, 1')$ are not independent, hence in his original paper ([KELDYSH, 1964](#)) Keldysh performs a linear $\frac{\pi}{4}$ -rotation in the Schwinger-Keldysh space,

$$\hat{G} \rightarrow L\hat{G}L^\dagger, \quad (2.89)$$

where

$$L = \frac{1}{\sqrt{2}} \begin{bmatrix} 1 & -1 \\ 1 & 1 \end{bmatrix}. \quad (2.90)$$

The rotated matrix is

$$\hat{G} = \frac{1}{2} \begin{bmatrix} G - G^< - G^> + \tilde{G} & G - G^> + G^< - \tilde{G} \\ G - G^< + G^> - \tilde{G} & G + \tilde{G} + G^> + G^< \end{bmatrix}. \quad (2.91)$$

To proceed further we recall some identities[¶] from section (2.4)

$$G^R(1, 1') = \theta(\tau - \tau')(G^>(1, 1') - G^<(1, 1')). \quad (2.92)$$

One cannot know which contour variable is further in the contour. Hence, we have to consider the possibilities of either $\tau > \tau'$ or $\tau' > \tau$. Say we choose $\tau > \tau'$, by looking back at Eqs. (2.7) and (2.11), one notice that $G^> = G$ and $G^< = \tilde{G}$. Therefore according to Eq.(2.92)

$$G^R(1, 1') = G(1, 1') - G^<(1, 1') = G^>(1, 1') - \tilde{G}(1, 1'). \quad (2.93)$$

By doing the exactly same kind of analyzes and using the identities from section 2.4, one encounters the matrix

$$\hat{G} = \begin{bmatrix} 0 & G^A \\ G^R & G^K \end{bmatrix}. \quad (2.94)$$

So far we've been working with contour variables, eventually we have to come back to the real time dependency of the Green's functions. This can be easily done by considering

$$\int d\tau = \overbrace{\int_{-\infty}^{\infty} dt}^{\text{Forward branch}} + \overbrace{\int_{\infty}^{-\infty} dt}^{\text{Backward branch}} = \int_{-\infty}^{\infty} dt - \int_{-\infty}^{\infty} dt. \quad (2.95)$$

Therefore, Eq. (2.82) is written for matrix ij -component

$$\hat{G}_{ij}^1(1, 1') = \int d\mathbf{r}_2 \int_{-\infty}^{\infty} dt_2 \hat{G}_{i1}^0(1, 2)V(2)\hat{G}_{1j}^0(2, 1') - \int d\mathbf{r}_2 \int_{-\infty}^{\infty} dt_2 \hat{G}_{i2}^0(1, 2)V(2)\hat{G}_{2j}^0(2, 1'). \quad (2.96)$$

Introducing the dynamics index space or Keldysh index

$$\hat{V}(2) = V(2)\sigma_z, \quad (2.97)$$

where σ_z is the Pauli matrix which absorbs the minus sign in Eq. (2.96), thus, it is changed to a more compact form

$$\hat{G}_{ij}^1(1, 1') = \int d\mathbf{r}_2 \int_{-\infty}^{\infty} dt_2 \hat{G}_{ik}^0(1, 2)\hat{V}(2)_{kk'}\hat{G}_{k'j}^0(2, 1'). \quad (2.98)$$

[¶]Notice that we are now using contour instead of time variables.

The Dyson equation for Green's function in a matrix form is written as

$$\hat{G}^1 = \hat{G}_0 \hat{V} \hat{G}_0. \quad (2.99)$$

One realizes that by going to the Keldysh space and performing a rotation, Eq.(2.99) is the first-order term of a lookalike Dyson equation. Hence we can write a new Dyson equation, however, this time within the Keldysh space

$$\hat{G} = \hat{G}_0 + \hat{G}_0 \hat{V} \hat{G}. \quad (2.100)$$

Although we were able to make things much easier, there is a more convenient way to represent \hat{G} , introduced by Larkin and Ovchinnikov ([LARKIN; OVCHINNIKOV, 1975](#)), which gives us the simplest matrix representation of the propagator in the Keldysh space. To obtain it, we perform another rotation in a matrix defined as

$$\check{G} \equiv \sigma_z \hat{G} \quad (2.101)$$

and the rotation**

$$G \equiv L \check{G} L^\dagger, \quad (2.102)$$

yields the matrix

$$G = \begin{bmatrix} G^R & G^K \\ 0 & G^A \end{bmatrix}, \quad (2.103)$$

this representation is one way to obtain the quantum kinetic equations.

2.12. Non-equilibrium Dyson equation

From the last section we have worked with the potential V and we've also seen that a more general way to describe a system is to consider the self-energy. The position and time dependency of Σ , allows one to write Σ in the Keldysh space. The same analyses as for the Green's functions in section 2.11 is done for $\Sigma(\mathbf{r}, t, \mathbf{r}', t')$

$$\Sigma(\mathbf{r}, t, \mathbf{r}', t') = \begin{cases} \Sigma^<(\mathbf{r}, t, \mathbf{r}', t') & t' > t \\ \Sigma^>(\mathbf{r}, t, \mathbf{r}', t') & t > t' \end{cases}. \quad (2.104)$$

**Notice that we lose the $\hat{}$ notation for matrices

and also

$$\Sigma^R(\mathbf{r}, t, \mathbf{r}', t') = \theta(t - t')(\Sigma^>(\mathbf{r}, t, \mathbf{r}', t') - \Sigma^<(\mathbf{r}, t, \mathbf{r}', t')), \quad (2.105)$$

$$\Sigma^A(\mathbf{r}, t, \mathbf{r}', t') = \theta(t' - t)(\Sigma^<(\mathbf{r}, t, \mathbf{r}', t') - \Sigma^>(\mathbf{r}, t, \mathbf{r}', t')), \quad (2.106)$$

$$\Sigma^K(\mathbf{r}, t, \mathbf{r}', t') = \Sigma^>(\mathbf{r}, t, \mathbf{r}', t') + \Sigma^<(\mathbf{r}, t, \mathbf{r}', t'). \quad (2.107)$$

Mostly important, we are also able to write Σ in the triagonal representation

$$\Sigma = \begin{bmatrix} \Sigma^R & \Sigma^K \\ 0 & \Sigma^A \end{bmatrix}. \quad (2.108)$$

With the triagonal representation we are able to derive Dyson's equations for the Keldysh space. Start by G_0

$$G_0 = \begin{bmatrix} G_0^R & G_0^K \\ 0 & G_0^A \end{bmatrix}. \quad (2.109)$$

The general Dyson matrix equation is

$$G = G_0 + G_0 \Sigma G, \quad (2.110)$$

and replacing for the triagonal representation

$$\begin{bmatrix} G^R & G^K \\ 0 & G^A \end{bmatrix} = \begin{bmatrix} G_0^R & G_0^K \\ 0 & G_0^A \end{bmatrix} + \begin{bmatrix} G_0^R & G_0^K \\ 0 & G_0^A \end{bmatrix} \begin{bmatrix} \Sigma^R & \Sigma^K \\ 0 & \Sigma^A \end{bmatrix} \begin{bmatrix} G^R & G^K \\ 0 & G^A \end{bmatrix}. \quad (2.111)$$

For the G^R and G^A components we have respectively

$$G^R = G_0^R + G_0^R \Sigma^R G^R, \quad (2.112)$$

$$G^A = G_0^A + G_0^A \Sigma^A G^A. \quad (2.113)$$

The Keldysh component is

$$G^K = G_0^K + G_0^R \Sigma^R G^K + G_0^R \Sigma^K G^A + G_0^K \Sigma^A G^A. \quad (2.114)$$

With the Keldysh space we have been able to write the Dyson equations in a matrix form. The components of the Green's function gives rise to three non-equilibrium Dyson equations. In the next chapter we shall see how one can obtain the BTE from these components.

3 Kinetic Equations

We have chosen to write it in separated chapter that what is the cornerstone of our work, the Boltzmann transport equation. A deeper understanding is essential to apply the BTE for the kind of system we are interested in. We first present a spinless equation, easily found in the literature (RAMMER, 2007) and (HAUG; JAUHO, 2008). This is a systematic derivation and we'll see how important was to built the formalism rigorously. It turns out, that including spin is quite simple for the left-hand side (drift-diffusion) and a bit trickier for the right-hand side (collision integral). With a few approximations we derive a more general form of the BTE including spin, paving the way to applications in condensed matter physics.

3.1. Left-right subtracted Dyson's equation

During the derivation of the Dyson equation in section 2.1, we have placed in evidence to the left G_0V in Eq. (2.37), however, we could also have chosen VG_0 to the right, forming a different type of Dyson equation. As matter of fact, there are two ways to write Eq. (2.110), here in the matrix form as shown in table 3

Left Dyson equation	Right Dyson equation
$G = G_0 + G\Sigma G_0$	$G = G_0 + G_0\Sigma G$

Table 3 – Dyson equations

In order to obtain a kinetic equation one must subtract the two equations. Rewriting the right Dyson equation as

$$G = G_0 + G_0\Sigma G, \quad (3.1)$$

$$G_0^{-1}G - \Sigma G = \delta(1 - 1'). \quad (3.2)$$

Doing exactly same thing for the left Dyson equation and then subtracting, we get the so-called left-right subtracted Dyson equation

$$[G_0^{-1} - \Sigma, G]_c = 0. \quad (3.3)$$

The commutator and anti-commutator are given respectively by

$$[A, B]_c = A \otimes B - B \otimes A, \quad (3.4)$$

$$\{A, B\}_c = A \otimes B + B \otimes A. \quad (3.5)$$

The subscript c indicates convolution, along with the symbol \otimes

$$A \otimes B(1, 1') = \int dx_2 \int_{-\infty}^{\infty} dt_2 A(1, 2) B(2, 1'). \quad (3.6)$$

One define the functions

$$A(1, 1') \equiv i(G^R(1, 1') - G^A(1, 1')), \quad (3.7)$$

$$\text{Re } G(1, 1') \equiv \frac{1}{2}(G^R(1, 1') + G^A(1, 1')), \quad (3.8)$$

$$\Gamma(1, 1') \equiv i(\Sigma^R(1, 1') - \Sigma^A(1, 1')), \quad (3.9)$$

$$\text{Re } \Sigma(1, 1') \equiv \frac{1}{2}(\Sigma^R(1, 1') + \Sigma^A(1, 1')), \quad (3.10)$$

where $\text{Re } G$ and $\text{Re } \Sigma$ are related to renormalization effects and won't play a role in the BTE derivation (RAMMER, 2007), A is the well known spectral function and Γ is related to the collision rate of a particle as we shall see (KADANOFF, 2018). Therefore, Eq. (3.3) can be written in another very elegant and useful way by taking only the Keldysh component G^K out of the triangular matrix

$$[G_0^{-1} - \text{Re } \Sigma, G^K]_c - [\Sigma^K, \text{Re } G]_c = \frac{i}{2} \{ \Sigma^K, A \}_c - \frac{i}{2} \{ \Gamma, G^K \}_c. \quad (3.11)$$

Equation (3.11) gives birth to the BTE, the left-hand side will be responsible for diffusion and drift terms, while the right-hand side is the so-called collision integral.

3.2. The Gradient Expansion

One interested in deriving the BTE wish to see how the distribution function change over time, i.e., the scattering in and out of a volume in the phase space. However, due to the uncertainty principle, we're not interested in determining the accurate position a particle, otherwise we wouldn't be able to determine the momentum (KADANOFF, 2018). Thus, we consider that the disturbance changing the the distribution function vary slowly over macroscopic distances, enabling one to determine also the momentum, at a cost of working with macroscopic variables (RAMMER; SMITH, 1986). Therefore, we use Wigner coordinates

$$\mathbf{R} = \frac{\mathbf{r}_1 + \mathbf{r}_{1'}}{2}, \quad \mathbf{r} = \mathbf{r}_1 - \mathbf{r}_{1'}, \quad (3.12)$$

$$\mathbf{T} = \frac{t_1 + t_{1'}}{2}, \quad t = t_1 - t_{1'}, \quad (3.13)$$

and the compact notation introduced by (RAMMER, 2007),

$$X = (T, \mathbf{R}), \quad x = (t, \mathbf{r}), \quad (3.14)$$

$$p = (E, \mathbf{k}), \quad xp = -Et + \mathbf{k} \cdot \mathbf{r}. \quad (3.15)$$

The variables (\mathbf{r}, t) describes the microscopic properties of the system and (\mathbf{R}, T) a shift of the reference frame to the center-of-mass system, describing the macroscopic properties ruled by the non-equilibrium features of the state under consideration (RAMMER; SMITH, 1986).

According to the Appendix D, the convolution form of Eq.(3.3) in the Wigner coordinates are

$$(A \otimes B)(X, p) = e^{\frac{i}{2}(\partial_X^A \partial_p^B - \partial_p^A \partial_X^B)} A(X, p) B(X, p). \quad (3.16)$$

One now performs the so-called gradient expansion, which consists in an expansion up to first order of the exponential function in Eq. (3.16)

$$(A \otimes B)(X, p) \approx A(X, p) B(X, p) + \frac{i}{2} (\partial_X^A A(X, p) \partial_p^B B(X, p)) - \frac{i}{2} (\partial_p^A A(X, p) \partial_X^B B(X, p)), \quad (3.17)$$

therefore, the (anti-) commutators in Eq.(3.3),

$$i[A, B]_c = [A \otimes B]_p, \quad (3.18)$$

$$\{A, B\}_c = AB + BA. \quad (3.19)$$

The subscript p indicates that we are dealing with the commutator in Wigner coordinates. It also recalls the resemblance of the commutator written in such coordinates, to the Poisson bracket of classical mechanics due to

$$[A \otimes B]_p = (\partial_X^A \partial_p^B - \partial_p^A \partial_X^B) A(X, p) B(X, p), \quad (3.20)$$

$$[A \otimes B]_p = \left(\partial_E^A \partial_T^B - \partial_T^A \partial_E^B - \nabla_{\mathbf{k}}^A \cdot \nabla_{\mathbf{R}}^B + \nabla_{\mathbf{R}}^A \cdot \nabla_{\mathbf{k}}^B \right) A(X, p) B(X, p). \quad (3.21)$$

We have in mind a Fermi system out of equilibrium induced by a slowly varying potential $V(R, T)$. Hence, the inverse Green's function is

$$G_0^{-1} = E - \varepsilon_{\mathbf{k}} - V(R, T) \quad (3.22)$$

where $\varepsilon_{\mathbf{k}} = \frac{\mathbf{k}^2}{2m}$ the energy of a single particle.

In a system with low impurity concentration, the self-energies are so small enable one to consider them as constants (RAMMER; SMITH, 1986). The commutators carrying $\text{Re} \Sigma$ and Σ^K on the left side of Eq.(3.11) vanishes, leaving only

$$[G_0^{-1} \otimes G^K]_p = \partial_T G^K(E, \mathbf{k}, \mathbf{R}, T) + \partial_E G^K(E, \mathbf{k}, \mathbf{R}, T) \partial_T V(R, T) + \nabla_{\mathbf{R}} G^K(E, \mathbf{k}, \mathbf{R}, T) \cdot \nabla_{\mathbf{k}} \varepsilon_{\mathbf{k}} - \nabla_{\mathbf{k}} G^K(E, \mathbf{k}, \mathbf{R}, T) \cdot \nabla_{\mathbf{R}} V(\mathbf{R}, T), \quad (3.23)$$

while the right hand side becomes

$$i\Sigma^K A - i\Gamma G^K. \quad (3.24)$$

Equation (3.23) will be responsible for the drift-diffusion equation and Eq.(3.24) will become the collision integral.

3.3. The quasi-particle approximation

We have assumed a very important approximation, of a dilute gas. It has led to the vanishing of some terms on the left hand side. By considering weak interactions we're doing the so-called quasi-particle approximation. To show what it means, we start from Eq.(2.50) and the Dyson equation for the retarded and advanced components*

$$G^R(E, \mathbf{k}, \mathbf{R}, T) = \frac{1}{G_0^{-1} - \Sigma^R}, \quad G^A(E, \mathbf{k}, \mathbf{R}, T) = \frac{1}{G_0^{-1} - \Sigma^A}. \quad (3.25)$$

subtracting both equations, using Eqs. (3.9), (3.10) and using

$$A(E, \mathbf{k}, \mathbf{R}, T) = i(G^R - G^A) = i(G^> - G^<) \quad (3.26)$$

we find a spectral function for the non-equilibrium case

$$A(E, \mathbf{k}) = \frac{\Gamma(E, \mathbf{k})}{(G_0^{-1} + \text{Re } \Sigma)^2 + (\Gamma/2)^2} \quad (3.27)$$

For the non-equilibrium case the spectral function has a Lorentzian function character. However, for the case of a small rate of collisions, i.e., small self-energies and weak interactions, the Γ function becomes small and $\text{Re } \Sigma$ turning the Lorentzian into a peaked function. Therefore, we approximate the spectral function to a Dirac delta

$$A(E, \mathbf{k}, \mathbf{R}, T) = 2\pi\delta(E - \varepsilon_{\mathbf{k}} - V(\mathbf{R}, T)). \quad (3.28)$$

$$A(E, \mathbf{k}, \mathbf{R}, T) = 2\pi\delta(E - G_0^{-1}). \quad (3.29)$$

From Eq.(3.28), the spectral function is peaked in the variable E very much alike the spectral function for the unperturbed case. This approximation physically means we are considering that between collisions, the electron moves as a free particle, suffering no interaction whatsoever (RAMMER, 2007).

For the equilibrium Green's functions we have similar relations to Ref. (BRUUS; FLENSBERG, 2004)

$$iG^>(E, \mathbf{k}, \mathbf{R}, T) = A(E, \mathbf{k}, \mathbf{R}, T)(1 - f_{\mathbf{k}}), \quad (3.30)$$

$$-iG^<(E, \mathbf{k}, \mathbf{R}, T) = A(E, \mathbf{k}, \mathbf{R}, T)f_{\mathbf{k}}, \quad (3.31)$$

The difference here is that f has variables $(\mathbf{k}, \mathbf{R}, T)$ and is a non-equilibrium distribution function. According to Eq.(2.17) and (3.28) the Keldysh component also has a Dirac delta character

$$G^K(E, \mathbf{k}, \mathbf{R}, T) = 2\pi i\delta(E - \varepsilon_{\mathbf{k}} - V(\mathbf{R}, T))(1 - 2f_{\mathbf{k}}). \quad (3.32)$$

*Note that according to Eq.(2.114) this is not valid for the Keldysh component.

therefore, if A is a peaked function so does G^K . It is useful to define a distribution function h

$$h(\mathbf{k}, \mathbf{R}, T) = -\frac{1}{2\pi i} \int_{-\infty}^{\infty} dE G^K, \quad (3.33)$$

so that

$$h = 1 - 2f_{\mathbf{k}}. \quad (3.34)$$

The distribution h is then related to the Keldysh component by

$$G^K = 2\pi i \delta(E - \varepsilon_{\mathbf{k}} - V(\mathbf{R}, T)) h. \quad (3.35)$$

One considering the quasi-particle approximation starts noticing that the equations for non-equilibrium takes similar forms of those for the equilibrium case.

3.4. The Boltzmann Equation

In this section we finally derive the BTE. One start by integrating $-\frac{1}{2\pi i} \int_{-\infty}^{\infty} dE$ in Eq.(3.23) and employing the quasi-particle approximation, the left-hand side yields

$$(\partial_T + \nabla_{\mathbf{k}} \varepsilon_{\mathbf{k}} \cdot \nabla_{\mathbf{R}} - \nabla_{\mathbf{R}} V(\mathbf{R}, T) \cdot \nabla_{\mathbf{k}}) h(\mathbf{k}, \mathbf{R}, T), \quad (3.36)$$

by integrating, the term carrying a derivative over E vanishes. Doing the same thing for the right-hand side in Eq.(3.24)

$$\Sigma^K(\varepsilon_{\mathbf{k}} + V(\mathbf{R}, T), \mathbf{k}, \mathbf{R}, T) - \Gamma(\varepsilon_{\mathbf{k}} + V(\mathbf{R}, T), \mathbf{k}, \mathbf{R}, T) h(\mathbf{k}, \mathbf{R}, T). \quad (3.37)$$

There's still need to evaluate the term responsible for the collision integral, Eq.(3.37). The self-energies can take a vast array of forms responsible for infinity ways of interactions. We consider the simplest case, the impurity scattering. It consists of a short-ranged disorder potential $V(\mathbf{r}) = \sum_i v_0 \delta(\mathbf{r} - \mathbf{R}_i)$ from (SHEN; RAIMONDI; VIGNALE, 2014). \mathbf{R}_i is the position of impurities placed randomly in the system having an average density n_i . One has to compute the impurity average as in reference (RAMMER, 2018) and take the so-called born approximation. The *zeroth* order self-energy diagram is given by (??)

$$\Sigma_0 = \begin{array}{c} \text{---} \\ \diagup \quad \diagdown \\ \text{---} \end{array} \quad (3.38)$$

$$\Sigma_0(E, \mathbf{k}, \mathbf{R}, T) = n_i v_0^2 \sum_{\mathbf{k}'} G(E, \mathbf{k}', \mathbf{R}, T). \quad (3.39)$$

Once the self-energies are defined, one has to compute the Γ and Σ^K functions. We recall the relations (3.9) and (3.7)

$$\Gamma(\varepsilon_{\mathbf{k}} + V(\mathbf{R}, T), \mathbf{k}, \mathbf{R}, T) = i \left[\Sigma^R(\varepsilon_{\mathbf{k}} + V(\mathbf{R}, T), \mathbf{k}', \mathbf{R}, T) - \Sigma^A(\varepsilon_{\mathbf{k}} + V(\mathbf{R}, T), \mathbf{k}', \mathbf{R}, T) \right], \quad (3.40)$$

$$= n_i v_0^2 \sum_{\mathbf{k}'} i \left[G^R(\varepsilon_{\mathbf{k}} + V(\mathbf{R}, T), \mathbf{k}', \mathbf{R}, T) - G^A(\varepsilon_{\mathbf{k}} + V(\mathbf{R}, T), \mathbf{k}', \mathbf{R}, T) \right], \quad (3.41)$$

$$= n_i v_0^2 \sum_{\mathbf{k}'} A(\varepsilon_{\mathbf{k}} + V(\mathbf{R}, T), \mathbf{k}', \mathbf{R}, T), \quad (3.42)$$

and according to the analytic expression for the self-energy

$$\Sigma_0^K(\varepsilon_{\mathbf{k}} + V(\mathbf{R}, T), \mathbf{k}, \mathbf{R}, T) = n_i v_0^2 \sum_{\mathbf{k}'} G^K(\varepsilon_{\mathbf{k}} + V(\mathbf{R}, T), \mathbf{k}', \mathbf{R}, T). \quad (3.43)$$

The functions A and G^K were discussed last section, they have a delta feature, similar to equilibrium. Therefore,

$$\Gamma(\varepsilon_{\mathbf{k}} + V(\mathbf{R}, T), \mathbf{k}, \mathbf{R}, T) = n_i v_0^2 \sum_{\mathbf{k}'} 2\pi \delta(\varepsilon_{\mathbf{k}} - \varepsilon_{\mathbf{k}'}), \quad (3.44)$$

$$\Sigma_0^K(\varepsilon_{\mathbf{k}} + V(\mathbf{R}, T), \mathbf{k}, \mathbf{R}, T) = n_i v_0^2 \sum_{\mathbf{k}'} 2\pi \delta(\varepsilon_{\mathbf{k}} - \varepsilon_{\mathbf{k}'}) h(\mathbf{k}', \mathbf{R}, T). \quad (3.45)$$

Replacing these results in Eqs.(3.36) and (3.37)

$$(\partial_T + \nabla_{\mathbf{k}} \varepsilon_{\mathbf{k}} \cdot \nabla_{\mathbf{R}} - \nabla_{\mathbf{R}} V(\mathbf{R}, T) \cdot \nabla_{\mathbf{k}}) h(\mathbf{k}, \mathbf{R}, T) = -2\pi n_i v_0^2 \sum_{\mathbf{k}'} \delta(\varepsilon_{\mathbf{k}} - \varepsilon_{\mathbf{k}'}) (h(\mathbf{k}, \mathbf{R}, T) - h(\mathbf{k}', \mathbf{R}, T)). \quad (3.46)$$

One can also write the BTE using the more familiar distribution function presented in Eq.(3.33)

$$(\partial_T + \nabla_{\mathbf{k}} \varepsilon_{\mathbf{k}} \cdot \nabla_{\mathbf{R}} - \nabla_{\mathbf{R}} V(\mathbf{R}, T) \cdot \nabla_{\mathbf{k}}) f_{\mathbf{k}} = -2\pi i n_i v_0^2 \sum_{\mathbf{k}'} \delta(\varepsilon_{\mathbf{k}} - \varepsilon_{\mathbf{k}'}) (f_{\mathbf{k}} - f_{\mathbf{k}'}). \quad (3.47)$$

$$(\partial_T + \nabla_{\mathbf{k}} \varepsilon_{\mathbf{k}} \cdot \nabla_{\mathbf{R}} - \nabla_{\mathbf{R}} V(\mathbf{R}, T) \cdot \nabla_{\mathbf{k}}) f_{\mathbf{k}} = I_{coll} \quad (3.48)$$

It should be clear that the BTE assume many forms, altered either by the choice of the Hamiltonian and/or by the type of interaction. The self-energy for impurity scattering have higher order terms that gives rise to more collision integrals (SHEN; RAIMONDI; VIGNALE, 2014). Nonetheless, to derive the BTE for this simple case and using the Keldysh formalism sets the stage to easily introduce modifications so that one can describe the system in mind, as we shall see in the next section when spin is included.

3.5. The Quantum Spin Boltzman Equation

In this dissertation we introduce the non-equilibrium formalism aiming to investigate spin-dependent phenomena. Mastering this formalism pays off when it comes to introduce corrections to the BTE derived and actually get physical results. We have determined the spinless transport Boltzmann equation, the good news is, to include the spin drift-diffusion, for now, we only work on the left hand side of Eq.(3.47), however, an approximation has to be made and will be discussed bellow.

In the first chapter we've seen that the inverse Green's functions carries the Hamiltonian

$$G_0^{-1} = E - H \quad (3.49)$$

where $H = \varepsilon_{\mathbf{k}} + H_{\mathbf{k}}^{soc} + H_{\mathbf{r}} = H_{\mathbf{k}} + H_{\mathbf{r}}$. $H_{\mathbf{k}}^{soc}$ is the Hamiltonian responsible for the spin-orbit interaction. One replaces the inverse Green's function to Eqs.(3.17) and (3.23)

$$\begin{aligned} [G_0^{-1} \otimes G^K]_p &= G_0^{-1}(X, p)G^K(X, p) + \frac{i}{2} \left(\partial_X G_0^{-1}(X, p) \partial_p G^K(X, p) \right) - \frac{i}{2} \left(\partial_p G_0^{-1}(X, p) \partial_X G^K(X, p) \right) \\ &\quad - G^K(X, p)G_0^{-1}(X, p) - \frac{i}{2} \left(\partial_X G^K(X, p) \partial_p G_0^{-1}(X, p) \right) + \frac{i}{2} \left(\partial_p G^K(X, p) \partial_X G_0^{-1}(X, p) \right), \end{aligned} \quad (3.50)$$

$$\begin{aligned} [G_0^{-1} \otimes G^K]_p &= G_0^{-1}G^K + \frac{i}{2} \left(-\partial_T G_0^{-1} \partial_E G^K + \nabla_{\mathbf{R}} G^K \cdot \nabla_{\mathbf{k}} G_0^{-1} \right) \\ &\quad - \frac{i}{2} \left(-\partial_E G_0^{-1} \partial_T G^K + \nabla_{\mathbf{k}} G_0^{-1} \cdot \nabla_{\mathbf{R}} G^K \right) \\ &\quad - G^K G_0^{-1} - \frac{i}{2} \left(-\partial_T G^K \partial_E G_0^{-1} + \nabla_{\mathbf{R}} G_0^{-1} \cdot \nabla_{\mathbf{k}} G^K \right) \\ &\quad + \frac{i}{2} \left(-\partial_E G^K \partial_T G_0^{-1} + \nabla_{\mathbf{k}} G^K \cdot \nabla_{\mathbf{R}} G_0^{-1} \right). \end{aligned} \quad (3.51)$$

by integrating over E according to Eq.(3.33) some of the the derivatives vanishes and using Eqs.(3.34) and (3.49) we obtain

$$\partial_t f_{\mathbf{k}} + i[H_{\mathbf{k}}, f_{\mathbf{k}}] + \frac{1}{2} \{ \nabla_{\mathbf{k}} H_{\mathbf{k}}, \nabla_{\mathbf{r}} f_{\mathbf{k}} \} - \frac{1}{2} \{ \nabla_{\mathbf{r}} H_{\mathbf{r}}, \nabla_{\mathbf{k}} f_{\mathbf{k}} \} = I_{\mathbf{k}}. \quad (3.52)$$

Eq (3.52) is the Spin Transport Boltzmann equation. By considering a spin-orbit part in the Hamiltonian, the left-hand side get additional terms. As for the right hand side, when one consider the quasi-particle approximation, the denominator Eq. (3.27) carries G_0^{-1} . Therefore, the delta function in Eq.(3.28) should also carry the additional spin-orbit Hamiltonian term. However, the effects of $H_{\mathbf{k}}^{soc}$ are so small compared to the other terms of the Hamiltonian that we choose to retain the gradient approximation as if nothing had changed on the right hand side. Although is a bold assumption, it produces good results to the end of our main research interest[†].

[†]To a reader interested, Ref. (SHEN; RAIMONDI; VIGNALE, 2014) overcome this problem. However, this process yields more terms in the collision integral that we are not interested here.

In order to give a familiar face to the SBTE, we have changed the \mathbf{R} and T variables to \mathbf{r} and t , respectively. Notice that this is just a change of notation, \mathbf{r} and t are still center of mass variables.

Obtaining Eq. (3.52) was definitely a formidable task. However, so far one has only taken the first step towards its application on a whole variety of systems, which may range far beyond spin-dependent phenomena.

4 Applications and Results

In this chapter we show one of the possible applications for the formalism presented before. On the first section we solve the Hamiltonian for a GaAs system considering the Rashba and Dresselhaus spin-orbit interaction. Then we discuss how to obtain the drift and diffusion equations for the PSH regime. This lead to an important result we've achieved. We have been able to also derive a drift-diffusion equation for two subbands and solved for the so-called crossed PSH regime.

4.1. 2D GaAs Quantum well

A crystallographic inversion asymmetry and an external electrical field gives rise to the Dresselhaus and Rashba spin orbit interactions ([DRESSELHAUS, 1955](#)). The GaAs system is such that the conduction band has a discontinuity forming a quantum well as shown in figure 8 a). For the one subband case we have to solve the hamiltonian

$$H = \frac{\mathbf{p}^2}{2m} + H_{\text{Rashba}} + H_{\text{Dresselhaus}}, \quad (4.1)$$

where the Rashba and Dresselhaus contributions are respectively given by

$$H_{\text{Rashba}} = \alpha(\sigma_x k_y - \sigma_y k_x), \quad (4.2)$$

$$H_{\text{Dresselhaus}} = \beta(\sigma_x k_y + \sigma_y k_x). \quad (4.3)$$

The Hamiltonian in Eq. 4.1 gives rise to energy subbands as depicted in figure 8 b).

The PSH arises in two situations, when $\alpha = \beta$ or $\alpha = -\beta$. For the first case, the Hamiltonian simplifies to

$$H = \frac{\hbar^2 \mathbf{k}^2}{2m} + 2\alpha \sigma_x k_y. \quad (4.4)$$

Diagonalizing it, we find the eigenvalues

$$\epsilon_{\pm} = \frac{\hbar^2 \mathbf{k}^2}{2m} \pm 2\alpha k_y. \quad (4.5)$$

The Hamiltonian in Eq.(4.4) commutes with σ_x for all \mathbf{k} , therefore the eigenstates of σ_x are also eigenstates of H . These eigenstates are illustrated in the k-space diagram in figure 8 c) creating a vertical pattern. For the case where $\alpha = -\beta$, the results are similar, but the resulting pattern is horizontal.

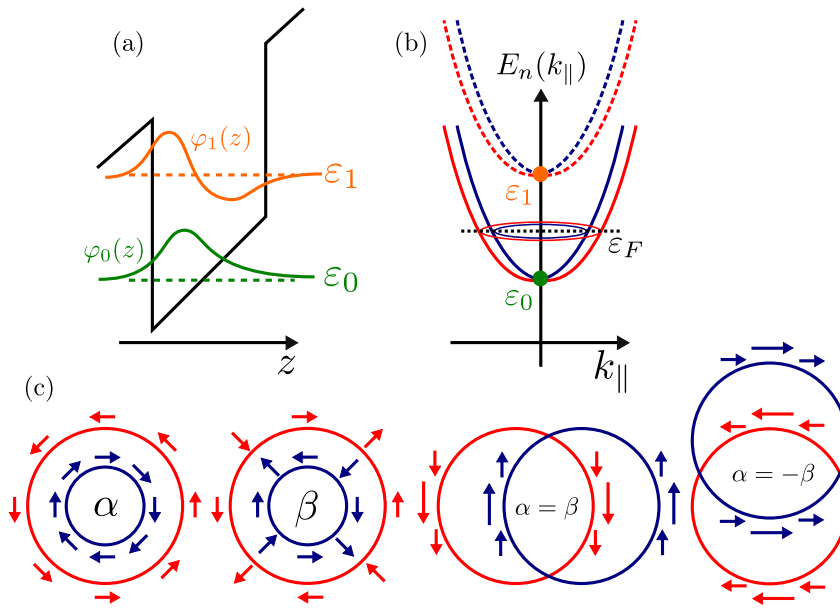


Figure 8 – a) A quantum well formed in the GaAs with an electric field inducing the Rashba spin-orbit interaction α . b) The subbands arising as solution to the Schrödinger equation. c) The spin eigenstates plotted in k -space for a Hamiltonian containing respectively only Rashba, only Dresselhaus and in the uniaxial regime ($\alpha = \beta$), which will lead to the PSH.

4.2. Drift-Diffusion Equations

In this section we derive a very important result from the SBTE, the *drift-diffusion equations*. We point out that if one wants a more general equation for impurity scattering, other terms for the collision integral have to be considered, as in reference (SHEN; RAIMONDI; VIGNALE, 2014). Once more orders of the impurity self-energy are accounted (RAIMONDI et al.,), more collision integrals appear, for instance, terms responsible for impurity spin-orbit coupling. In this dissertation we consider the simplest case of the zeroth order (in the SOC intensity) and we shall work separately in the right and left hand sides. We will compute the angular average in both sides, starting by the collision integral. The sum over the vector $\mathbf{k}' = (k, \theta')$ is turned into a sum over the modulo k' and the angular component θ'

$$\sum_{\mathbf{k}'} \rightarrow \sum_{k'} \sum_{\theta'} \rightarrow \sum_{k'} \int \frac{d\theta'}{2\pi}, \quad (4.6)$$

where we keep a shorthand notation $\sum_{k'} = \int k' dk'$, therefore,

$$I_{\mathbf{k}} = -2\pi n_i v_0^2 \sum_{\mathbf{k}'} \int \frac{d\theta'}{2\pi} \delta(\varepsilon_{\mathbf{k}} - \varepsilon_{\mathbf{k}'}) (f_{\mathbf{k}',\theta'} - f_{\mathbf{k},\theta}). \quad (4.7)$$

Defining the time relaxation as shown in (RAMMER, 2007) and also the average

distribution function (SHEN; RAIMONDI; VIGNALE, 2014), respectively

$$\frac{1}{\tau_0} = 2\pi n_i v_0^2 \sum_{\mathbf{k}'} \delta(\varepsilon_{\mathbf{k}} - \varepsilon_{\mathbf{k}'}) = n_i m v_0^2, \quad (4.8)$$

$$\int \frac{d\theta'}{2\pi} f_{k',\theta'} = \langle f_{k',\theta'} \rangle = f_k, \quad (4.9)$$

the collision integral becomes

$$I_{\mathbf{k}} = -\frac{f_{\mathbf{k}} - f_k}{\tau_0}. \quad (4.10)$$

Notice that we haven't taken the angular average in the first term yet.

We wish to compute an equation that describes how spin densities evolve with time. The trick to find such equation consists in expanding the distribution function accordingly $f_{\mathbf{k}} = g_{\mathbf{k}}^i \sigma_i$ and $f_k = g_k^i \sigma_i$, with $i = 0, x, y, z$. The σ_0 is a 2×2 identity matrix and $g_{\mathbf{k}}^0$ is the charge distribution regardless of spin orientation (SHEN; RAIMONDI; VIGNALE, 2014).

For the left-hand side we consider the general Hamiltonian and the notation as in reference (SHEN; RAIMONDI; VIGNALE, 2014)

$$H = \varepsilon_{\mathbf{k}} + H_{\mathbf{k}}^{soc} + H(\mathbf{r}) \quad (4.11)$$

where*

$$\varepsilon_{\mathbf{k}} = \frac{\mathbf{k}^2}{2m} \quad H_{\mathbf{k}}^{soc} = \sum_i \frac{k_i}{m} A_i^j \sigma_j \quad H(\mathbf{r}) = e\mathbf{E} \cdot \mathbf{r} \quad (4.12)$$

The sum runs over the index $i = x, y, z$, e is the electron charge, \mathbf{E} is an external electrical field and A_i^j are the components of a spin-dependent vector potential that describes the spin-orbit interaction with the crystal lattice. The vector potential is defined as

$$\begin{aligned} A_x^y &= m\lambda_1, & A_y^x &= m\lambda_2 \\ A_x^z &= m\alpha' e E_y, & A_y^z &= -m\alpha' e E_x \end{aligned} \quad (4.13)$$

where $\lambda_1 = \alpha + \beta$ and $\lambda_2 = \alpha - \beta$. $\alpha' \equiv \frac{\lambda^2}{4}$ is the square of the effective Compton wavelength for the GaAs and it's essential for the extrinsic spin Hall effect (RAIMONDI; SCHWAB, 2010), a phenomena that we shall not study here. Therefore, we shall soon make $\alpha' = 0$, however, just to get a grasp of how a general left-hand side looks like accounting this number of terms, we keep it until otherwise. Expanding the distribution function

$$\partial_t (g_{\mathbf{k}}^i \sigma_i) + \frac{\mathbf{k}}{m} \cdot \nabla_{\mathbf{r}} g_{\mathbf{k}}^i \sigma_i + i \left[\sum_i \frac{k_i}{m} A_i^j \sigma_j, g_{\mathbf{k}}^i \sigma_i \right] + \frac{1}{2} \left\{ \sum_i \nabla_{\mathbf{k}} \frac{k_i}{m} A_i^j \sigma_j, \nabla_{\mathbf{r}} g_{\mathbf{k}}^i \sigma_i \right\} - e\mathbf{E} \cdot \nabla_{\mathbf{k}} g_{\mathbf{k}}^i \sigma_i = I_{\mathbf{k}} \quad (4.14)$$

*Notice we have made $\hbar = 1$.

and writing its components

$$\begin{aligned}
& \partial_t g_{\mathbf{k}}^0 \sigma_0 + \frac{\mathbf{k}}{m} \cdot \nabla_{\mathbf{r}} g_{\mathbf{k}}^0 \sigma_0 + i \left[\sum_i \frac{k_i}{m} A_i^j \sigma_j, g_{\mathbf{k}}^0 \sigma_0 \right] + \frac{1}{2} \left\{ \sum_i \nabla_{\mathbf{k}} \frac{k_i}{m} A_i^j \sigma_j, \nabla_{\mathbf{r}} g_{\mathbf{k}}^0 \sigma_0 \right\} - e \mathbf{E} \cdot \nabla_{\mathbf{k}} g_{\mathbf{k}}^0 \sigma_0 + \\
& \partial_t g_{\mathbf{k}}^x \sigma_x + \frac{\mathbf{k}}{m} \cdot \nabla_{\mathbf{r}} g_{\mathbf{k}}^x \sigma_x + i \left[\sum_i \frac{k_i}{m} A_i^j \sigma_j, g_{\mathbf{k}}^x \sigma_x \right] + \frac{1}{2} \left\{ \sum_i \nabla_{\mathbf{k}} \frac{k_i}{m} A_i^j \sigma_j, \nabla_{\mathbf{r}} g_{\mathbf{k}}^x \sigma_x \right\} - e \mathbf{E} \cdot \nabla_{\mathbf{k}} g_{\mathbf{k}}^x \sigma_x + \\
& \partial_t g_{\mathbf{k}}^y \sigma_y + \frac{\mathbf{k}}{m} \cdot \nabla_{\mathbf{r}} g_{\mathbf{k}}^y \sigma_y + i \left[\sum_i \frac{k_i}{m} A_i^j \sigma_j, g_{\mathbf{k}}^y \sigma_y \right] + \frac{1}{2} \left\{ \sum_i \nabla_{\mathbf{k}} \frac{k_i}{m} A_i^j \sigma_j, \nabla_{\mathbf{r}} g_{\mathbf{k}}^y \sigma_y \right\} - e \mathbf{E} \cdot \nabla_{\mathbf{k}} g_{\mathbf{k}}^y \sigma_y + \\
& \partial_t g_{\mathbf{k}}^z \sigma_z + \frac{\mathbf{k}}{m} \cdot \nabla_{\mathbf{r}} g_{\mathbf{k}}^z \sigma_z + i \left[\sum_i \frac{k_i}{m} A_i^j \sigma_j, g_{\mathbf{k}}^z \sigma_z \right] + \frac{1}{2} \left\{ \sum_i \nabla_{\mathbf{k}} \frac{k_i}{m} A_i^j \sigma_j, \nabla_{\mathbf{r}} g_{\mathbf{k}}^z \sigma_z \right\} - e \mathbf{E} \cdot \nabla_{\mathbf{k}} g_{\mathbf{k}}^z \sigma_z = I_{\mathbf{k}}
\end{aligned} \tag{4.15}$$

Next we use the commutation rules for the Pauli Matrices and the Fourier transform of $\partial_t = -i\omega$ and $\nabla_{\mathbf{r}} = iq_i$. We have to compute the commutator and the anti-commutator, starting by the first

$$i \left[\sum_i \frac{k_i}{m} A_i^j \sigma_j, g_{\mathbf{k}}^i \sigma_i \right] = -2 \frac{k_x}{m} A_x^z g_{\mathbf{k}}^x \sigma_y - 2 \frac{k_y}{m} A_y^z g_{\mathbf{k}}^x \sigma_y \tag{4.16}$$

$$+ 2 \frac{k_x}{m} A_x^y g_{\mathbf{k}}^x \sigma_z - 2 \frac{k_y}{m} A_y^x g_{\mathbf{k}}^y \sigma_z \tag{4.17}$$

$$+ 2 \frac{k_x}{m} A_x^z g_{\mathbf{k}}^y \sigma_x + 2 \frac{k_y}{m} A_y^z g_{\mathbf{k}}^y \sigma_x \tag{4.18}$$

$$- 2 \frac{k_x}{m} A_x^y g_{\mathbf{k}}^z \sigma_x + 2 \frac{k_y}{m} A_y^x g_{\mathbf{k}}^z \sigma_y \tag{4.19}$$

The anti-commutator part

$$\frac{1}{2} \left\{ \sum_i \nabla_{\mathbf{k}} \frac{k_i}{m} A_i^j \sigma_j, \nabla_{\mathbf{r}} g_{\mathbf{k}}^i \sigma_i \right\} = i A_y^x g_{\mathbf{k}}^x \sigma_0 + i A_x^y q_x g_{\mathbf{k}}^z \sigma_0 + i A_x^z q_x g_{\mathbf{k}}^z \sigma_0 \tag{4.20}$$

$$+ i A_y^z q_y g_{\mathbf{k}}^z \sigma_0 + \frac{i}{m} A_x^y q_x g_{\mathbf{k}}^0 \sigma_y + \frac{i}{m} A_x^z q_x g_{\mathbf{k}}^0 \tag{4.21}$$

$$+ \frac{i}{m} A_y^x q_y g_{\mathbf{k}}^0 \sigma_x + \frac{i}{m} A_y^z q_y g_{\mathbf{k}}^0 \sigma_z \tag{4.22}$$

By putting the Pauli Matrices in evidence, the left-hand-side becomes the Matrix

$$\begin{bmatrix}
\Omega & i\lambda_2 \tau_0 q_y & i\lambda_1 \tau_0 q_x & im\alpha'(\mathbf{q} \times \mathbf{v})_z \\
i\lambda_2 \tau_0 q_y & \Omega & 2\tau_0 e\alpha'(\mathbf{k} \times \mathbf{E})_z & -2\tau_0 k_x \lambda_1 \\
\lambda_1 \tau_0 q_x & -2\tau_0 e\alpha'(\mathbf{k} \times \mathbf{E})_z & \Omega & 2\tau_0 k_y \lambda_2 \\
im\alpha'(\mathbf{q} \times \mathbf{v})_z & 2\tau_0 k_x \lambda_1 & -2\tau_0 k_y \lambda_2 & \Omega
\end{bmatrix}
\begin{bmatrix}
g_{\mathbf{k}}^0 \\
g_{\mathbf{k}}^x \\
g_{\mathbf{k}}^y \\
g_{\mathbf{k}}^z
\end{bmatrix} = I_{\mathbf{k}} \tag{4.23}$$

where $\Omega = -i\omega\tau_0 + i\frac{\tau_0}{m}\mathbf{k} \cdot \mathbf{q} - e\tau_0\mathbf{E} \cdot \nabla_{\mathbf{k}}$. Notice that τ_0 comes from the denominator in Eq.(4.10). We have derived a more general drift and diffusion matrix, however, we're not

interested in the extrinsic spin-orbit interaction, thus, we shall consider the limit where it vanishes. Additionally, an external electrical field is neglected. Thus, $\alpha' = 0$ and $\mathbf{E} = 0$. Consequently, we obtain

$$\begin{bmatrix} \Omega & i\lambda_2\tau_0q_y & i\lambda_1\tau_0q_x & 0 \\ i\lambda_2\tau_0q_y & \Omega & 0 & -2\tau_0k_x\lambda_1 \\ \lambda_1\tau_0q_x & 0 & \Omega & 2\tau_0k_y\lambda_2 \\ 0 & 2\tau_0k_x\lambda_1 & -2\tau_0k_y\lambda_2 & \Omega \end{bmatrix} \begin{bmatrix} g_{\mathbf{k}}^0 \\ g_{\mathbf{k}}^x \\ g_{\mathbf{k}}^y \\ g_{\mathbf{k}}^z \end{bmatrix} = I_{\mathbf{k}} \quad (4.24)$$

The collision integral part when expanded, yields

$$I_{\mathbf{k}} = - \begin{bmatrix} g_{\mathbf{k}}^0 \\ g_{\mathbf{k}}^x \\ g_{\mathbf{k}}^y \\ g_{\mathbf{k}}^z \end{bmatrix} + \begin{bmatrix} g_k^0 \\ g_k^x \\ g_k^y \\ g_k^z \end{bmatrix} \quad (4.25)$$

where the matrices on the right is similarly denoted respectively by $\mathbf{g}_{\mathbf{k}}$ and \mathbf{g}_k .

Denoting the resulting matrix on the left hand side \mathcal{K} . The BTE (4.14) can be solved by

$$\mathcal{K}\mathbf{g}_{\mathbf{k}} = -\mathbf{g}_{\mathbf{k}} + \mathbf{g}_k \quad (4.26)$$

$$\mathbf{g}_{\mathbf{k}} = (I + \mathcal{K})^{-1}\mathbf{g}_k \quad (4.27)$$

where the subscript -1 indicates the matrix inverse. Moreover, we use the trick presented by Ref.(LIU; SINOVA, 2012) taking the angle average over \mathbf{k} one obtain a close equation for the averaged distribution function vector \mathbf{g}_k

$$\langle \mathbf{g}_{\mathbf{k}} \rangle = \langle (I + \mathcal{K})^{-1} \rangle \mathbf{g}_k \quad (4.28)$$

the $\langle \cdot \rangle$ means the angular average of θ .

We search a diffusion equation of the form

$$\partial_t \begin{bmatrix} N \\ S_x \\ S_y \\ S_z \end{bmatrix} = D(\mathbf{q}) \begin{bmatrix} N \\ S_x \\ S_y \\ S_z \end{bmatrix} \quad (4.29)$$

where the charge density is defined as $N = \sum_{\mathbf{k}} g_{\mathbf{k}}^0$ and the spin density $S_i = \sum_{\mathbf{k}} g_{\mathbf{k}}^i$.

Moreover, we define the two-dimensional diffusion constant $D = \tau_0 \frac{k_F^2}{2m^2}$. By taking the $-i\omega$ part out of Ω in Eq.(4.23), Fourier transforming back to real time and placing on the left hand side, and making the approximation $\frac{k_F q}{m}, |\lambda_i| k_F \ll E_F$, the matrix takes the form we were looking for

$$\partial_t \begin{bmatrix} N(\mathbf{q}, t) \\ S_x(\mathbf{q}, t) \\ S_y(\mathbf{q}, t) \\ S_z(\mathbf{q}, t) \end{bmatrix} = \begin{bmatrix} -D\mathbf{q}^2 & iq_y\lambda_2 & -iq_x\lambda_1 & 0 \\ -iq_y\lambda_2 & -D\mathbf{q}^2 - \frac{1}{\tau_x} & 0 & -4iDmq_x\lambda_1 \\ -iq_x\lambda_1 & 0 & -D\mathbf{q}^2 - \frac{1}{\tau_y} & 4iDmq_y\lambda_2 \\ 0 & 4iDmq_x\lambda_1 & -4iDmq_y\lambda_2 & -D\mathbf{q}^2 - \frac{1}{\tau_z} \end{bmatrix} \begin{bmatrix} N(\mathbf{q}, t) \\ S_x(\mathbf{q}, t) \\ S_y(\mathbf{q}, t) \\ S_z(\mathbf{q}, t) \end{bmatrix} \quad (4.30)$$

In Eq.(4.30) we have also defined the relaxation times

$$\frac{1}{\tau_x} = D4m^2\lambda_1^2 \quad (4.31)$$

$$\frac{1}{\tau_y} = D4m^2\lambda_2^2 \quad (4.32)$$

$$\frac{1}{\tau_z} = D4m^2(\lambda_1^2 + \lambda_2^2) = \frac{1}{\tau_x} + \frac{1}{\tau_y} \quad (4.33)$$

which comes from the Dyaknov-Perel mechanism.

4.3. Persistent Spin Helix (PSH)

Equation (4.30) now takes a beautiful and manageable form. Therefore, we shall use it to determine how the spin densities in the \hat{z} direction evolves with time in the PSH regime. Consider $\alpha = \beta$, thus, $\lambda_2 = 0$ and all the terms carrying it vanishes. The diffusion

equation for the PSH is then

$$\partial_t \begin{bmatrix} N(\mathbf{q}, t) \\ S_x(\mathbf{q}, t) \\ S_y(\mathbf{q}, t) \\ S_z(\mathbf{q}, t) \end{bmatrix} = \begin{bmatrix} -D\mathbf{q}^2 & 0 & -iq_x\lambda_1 & 0 \\ 0 & -D\mathbf{q}^2 + \frac{1}{\tau_x} & 0 & -4iDmq_x\lambda_1 \\ -iq_x\lambda_1 & 0 & -D\mathbf{q}^2 & 0 \\ 0 & 4iDmq_x\lambda_1 & 0 & -D\mathbf{q}^2 + \frac{1}{\tau_x} \end{bmatrix} \begin{bmatrix} N(\mathbf{q}, t) \\ S_x(\mathbf{q}, t) \\ S_y(\mathbf{q}, t) \\ S_z(\mathbf{q}, t) \end{bmatrix}, \quad (4.34)$$

where $v_1 = 4Dm\lambda_1$.

Eq.4.34 can be broken into

$$\partial_t \begin{bmatrix} S_x(\mathbf{q}, t) \\ S_z(\mathbf{q}, t) \end{bmatrix} = \begin{bmatrix} -D\mathbf{q}^2 - \frac{1}{\tau_x} & -iv_1q_x \\ iv_1q_x & -D\mathbf{q}^2 - \frac{1}{\tau_x} \end{bmatrix} \begin{bmatrix} S_x(\mathbf{q}, t) \\ S_z(\mathbf{q}, t) \end{bmatrix}, \quad (4.35)$$

and

$$\partial_t \begin{bmatrix} N(\mathbf{q}, t) \\ S_y(\mathbf{q}, t) \end{bmatrix} = \begin{bmatrix} -D\mathbf{q}^2 & i\lambda_1q_x \\ i\lambda_1q_x & -D\mathbf{q}^2 - \frac{1}{\tau_x} \end{bmatrix} \begin{bmatrix} N(\mathbf{q}, t) \\ S_y(\mathbf{q}, t) \end{bmatrix}. \quad (4.36)$$

We're interested in how the spin in \hat{z} direction behave. Thus, we take the first block and use the Ansatz

$$\begin{bmatrix} S_x(\mathbf{q}, t) \\ S_z(\mathbf{q}, t) \end{bmatrix} = \begin{bmatrix} s_x(\mathbf{q}, t) \\ s_z(\mathbf{q}, t) \end{bmatrix} e^{-(D\mathbf{q}^2 + \frac{1}{\tau_x})t}. \quad (4.37)$$

Replacing Eq.(4.37) into Eq.4.35

$$\partial_t \begin{bmatrix} s_x(\mathbf{q}, t) \\ s_z(\mathbf{q}, t) \end{bmatrix} = v_1q_x \begin{bmatrix} 0 & -i \\ i & 0 \end{bmatrix} \begin{bmatrix} s_x(\mathbf{q}, t) \\ s_z(\mathbf{q}, t) \end{bmatrix}, \quad (4.38)$$

$$\begin{bmatrix} s_x(\mathbf{q}, t) \\ s_z(\mathbf{q}, t) \end{bmatrix} = e^{v_1q_x\sigma_y t} \begin{bmatrix} s_x^0(\mathbf{q}, 0) \\ s_z^0(\mathbf{q}, 0) \end{bmatrix}. \quad (4.39)$$

Expanding the exponential we get

$$\begin{bmatrix} s_x(q_x, t) \\ s_z(q_x, t) \end{bmatrix} = \begin{bmatrix} \cosh(v_1q_x t) & -i\sinh(v_1q_x t) \\ i\sinh(v_1q_x t) & \cosh(v_1q_x t) \end{bmatrix} \begin{bmatrix} s_x^0(q_x, 0) \\ s_z^0(q_x, 0) \end{bmatrix}. \quad (4.40)$$

Taking $s_z^0 = 1$ and $s_x^0 = 0$, i.e., in the \hat{z} direction the spins are up and down in the \hat{x} direction. Imposing the initial condition the equation gives

$$S_x(\mathbf{q}, t) = -ie^{-Dt\mathbf{q}^2} e^{-\frac{t}{\tau_x}} \sinh(v_1 q_x t), \quad (4.41)$$

$$S_z(\mathbf{q}, t) = -ie^{-Dt\mathbf{q}^2} e^{-\frac{t}{\tau_x}} \cosh(v_1 q_x t). \quad (4.42)$$

We wish to see how the spin evolves in \hat{z} , hence, taking the inverse Fourier transform of q components of $S_z(\mathbf{q}, t)$

$$e^{-Dtq_y^2} \rightarrow \frac{e^{-\frac{y^2}{4Dt}}}{\sqrt{2Dt}}, \quad (4.43)$$

$$e^{-Dtq_x^2} \cosh(v_1 q_x t) \rightarrow \frac{e^{-\frac{x^2}{4Dt}}}{\sqrt{2Dt}} e^{\frac{tv_1^2}{4D}} \cos\left(\frac{v_1 x}{2D}\right). \quad (4.44)$$

The time evolution of the spin densities in the \hat{z} direction is given by the equation

$$S_z(\mathbf{r}, t) = \frac{e^{-\frac{r^2}{4Dt}}}{2Dt} \cos(\kappa x), \quad (4.45)$$

where $\kappa = \frac{v_1}{2D}$.

One notice that the term responsible for time relaxation vanishes, remaining only two terms on the right hand side. The first responsible for diffusion and the second for the spin precession. This result presents a beautiful pattern as depicted in figure 9.

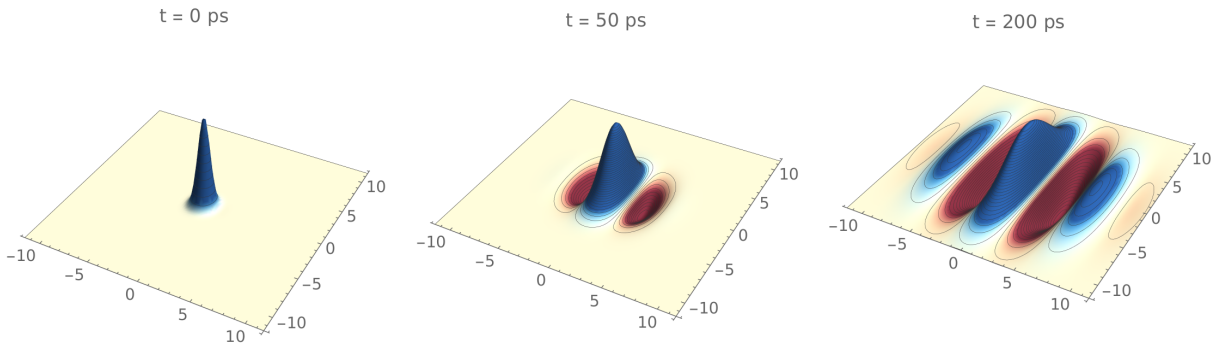


Figure 9 – The time evolution of the spin polarization in the \hat{z} direction. The blue color represents spin up and red color spin down.

The interesting thing about the PSH regime is that although we have considered the integral collision and a non-ballistic approach, there's no relaxation time for the regime and the spin polarization evolves in time creating the pattern presented in figure 9.

Sure is a long way to derive these results, however, approaching this kind of system based in a elegant and essential formalisms, such Keldysh and non-equilibrium Green's

function, one is able to build a strong foundation to analyze difficult systems that they wouldn't otherwise.

4.4. The drift-diffusion equation for two subbands

In this section is presented a recent preliminary result we've achieved by implementing all the tools and formalism learned writing this thesis. The mathematical steps are not displayed in deeper details. The extra complexity of the two-subband systems lead to long cumbersome equations that have been manipulated using the Wolfram Mathematica software. Instead, we choose to show only a summary of the necessary steps to reproduce these results, and a general discussion. We have also solved it numerically for the PSH regime. Our results show divergences with respect to the current literature (FU et al., 2016), where a heuristic analysis of the two-subbands problem is introduced. Indeed we find that the two-subband PSH might fall into two possible regimes regarding the interband coupling, which matches and formalizes the discussion of (FERREIRA et al., 2017). The results of (FU et al., 2016) are only partially recovered for large spin-orbit couplings and very clean samples (large τ_0). However, as we'll see next, the complexity of the two-subbands problem require numerical analysis, thus the conclusions drawn here are only preliminary and a more detailed discussion will be the focus on a future publication.

The fundamental character playing a role in the drift-diffusion equation is the self-energy. It's a key function in building the collision integral. Hence, if one were to include two subbands it should start by analyzing it. As a first result, we would like to keep it simple and consider again the scattering with scalar delta-impurities. Nonetheless, with the mathematical formalism presented, one is able to include (with a few adjustments) as many interactions as necessary.

In section 3.4 we had to take the impurity average of the propagator in order to determine the self-energy. For two-subbands the development is identical, but now we have to carry the subband label. Within the Born approximation, we calculate the impurity average of the second order scattering process to find

$$\langle V_{\mu_b, \mu_c}(k_b, k_c) V_{\mu_c, \mu_a}(k_c, k_a) \rangle = N \delta_{b,a} v_0^2 \langle P \rangle_{b,c}. \quad (4.46)$$

where $\langle P \rangle_{b,c} = \int dZ |\varphi_{\mu_b}(Z)|^2 |\varphi_{\mu_c}(Z)|^2$ is a structural factor that arises in the two-subbands case, and $\varphi_\mu(z')$ are the subband eigenstates due to the confinement along z . This will be discussed bellow. The variable Z is the component of the position vector of the impurity in the \hat{z} axis. We have also made a change of basis to $|j, k, \sigma\rangle = |\mu, k\rangle$ and μ carries the information about the spin σ and the subband j .

We're looking for a drift-diffusion equation in a GaAs system, such system forms a quantum well, and interestingly enough, for two subbands, the impurity average structure

now depends on the symmetry of the quantum well due to the Z integral in Eq. (4.46). Solving the Hamiltonian for an infinity quantum well yields eigenstates with sines and cosines. However, in order to have Rashba spin orbit interaction, an external electrical field has to be applied, deforming the quantum well. A numerical analysis of $\langle P \rangle_{b,c}$ is shown in Fig. 10 as a function of the electric field. For a symmetric quantum well it has a delta character as

$$\langle P \rangle_{b,c} = 1 + \frac{1}{2} \delta_{\mu_b, \mu_c}. \quad (4.47)$$

As expected the self-energy carries a matrix form due to the subband labeling

$$\Sigma = \begin{pmatrix} \Sigma_1 & 0 \\ 0 & \Sigma_2 \end{pmatrix}, \quad (4.48)$$

or

$$\Sigma_j = N v_0^2 \sum_{j_c, k_c} G_{j_c}(k_c) P_{j, j_c}, \quad (4.49)$$

where $G_{j_c}(k_c)$ are 2×2 matrices in spin space for each subband j .

Determining the self-energy for the two subband case, enables one to reconstruct the collision integral. We first demonstrate how some important functions take a matrix form in the two subbands case, for instance, the spectral function within the quasi-particle approximation is

$$A(E, \mathbf{k}, \mathbf{R}, T) = \begin{pmatrix} 2\pi\delta(E - \varepsilon_{1,\mathbf{k}} - V(\mathbf{R}, T))\mathcal{I}_{2 \times 2} & 0 \\ 0 & 2\pi\delta(E - \varepsilon_{2,\mathbf{k}} - V(\mathbf{R}, T))\mathcal{I}_{2 \times 2} \end{pmatrix}, \quad (4.50)$$

where the labels 1 and 2 in $\varepsilon_{\mathbf{k}}$ indicates the subband. Whilst for the Keldysh component off the Green's function

$$G^K(E, \mathbf{k}, \mathbf{R}, T) = \begin{pmatrix} 2\pi\delta(E - \varepsilon_{1,\mathbf{k}} - V(\mathbf{R}, T))h_1 & 0 \\ 0 & 2\pi\delta(E - \varepsilon_{2,\mathbf{k}} - V(\mathbf{R}, T))h_2 \end{pmatrix}, \quad (4.51)$$

where $h_1 \equiv h_1(E, \mathbf{k}, \mathbf{R}, T)$ and $h_2 \equiv h_2(E, \mathbf{k}, \mathbf{R}, T)$ are 2×2 matrix distribution functions in spin space analogous to the one defined in Eq. (3.33).

According to Eqs.(3.44) and (3.45) we encounter the collision integral for two

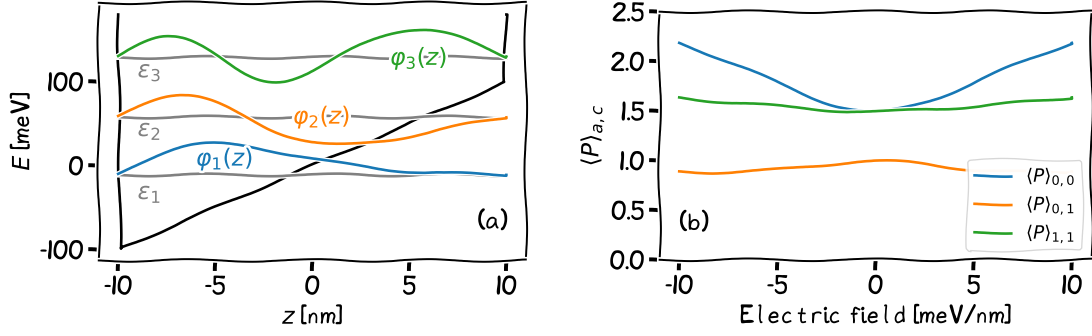


Figure 10 – (left) Wave-functions $\psi(z)$ for a tilted quantum well. (right) Result of $\langle P \rangle_{\mu_b, \mu_c, \mu_a}$ for different μ_b, μ_c combinations as a function of the electric field. Here $[b, c]$ range from the first subband (0) to the second (1). Everything is in arbitrary units. If needed, we have to fix the units properly.

subbands[†]

$$I_{\mathbf{k}} = \begin{pmatrix} \sum_{\theta'_1} \frac{1}{\tau_{11}} [f_{1, \mathbf{k}'} - f_{1, \mathbf{k}}] + \sum_{\theta'_2} \frac{1}{\tau_{12}} [f_{2, \mathbf{k}'} - f_{1, \mathbf{k}}] & 0 \\ 0 & \sum_{\theta'_2} \frac{1}{\tau_{22}} [f_{2, \mathbf{k}'} - f_{2, \mathbf{k}}] + \sum_{\theta'_1} \frac{1}{\tau_{21}} [f_{1, \mathbf{k}'} - f_{2, \mathbf{k}}] \end{pmatrix}. \quad (4.52)$$

We have defined

$$\frac{1}{\tau_{11}} = \sum_{k'_1} n_i v_0^2 2\pi \delta(\varepsilon_{\mathbf{k}_1} - \varepsilon_{\mathbf{k}'_1}) P_{11} = n_i m v_0^2 P_{11}, \quad (4.53)$$

$$\frac{1}{\tau_{12}} = \sum_{k'_2} n_i v_0^2 2\pi \delta(\varepsilon_{\mathbf{k}_1} - \varepsilon_{\mathbf{k}'_2}) P_{12} = n_i m v_0^2 P_{12}, \quad (4.54)$$

$$\frac{1}{\tau_{21}} = \sum_{k'_1} n_i v_0^2 2\pi \delta(\varepsilon_{\mathbf{k}_2} - \varepsilon_{\mathbf{k}'_1}) P_{21} = n_i m v_0^2 P_{21}, \quad (4.55)$$

$$\frac{1}{\tau_{22}} = \sum_{k'_2} n_i v_0^2 2\pi \delta(\varepsilon_{\mathbf{k}_2} - \varepsilon_{\mathbf{k}'_2}) P_{22} = n_i m v_0^2 P_{22}. \quad (4.56)$$

which can be summarized as $\tau_{jj'}^{-1} = \tau_0^{-1} P_{jj'}$. Therefore, the collision integral can be written

$$I_{\mathbf{k}} = \sum_{j_c} \frac{1}{\tau_0} \left[-f_{j, \mathbf{k}} + \langle f_{j_c, \mathbf{k}'} \rangle \right] P_{j, j_c}, \quad (4.57)$$

where the $\langle \cdot \rangle$ represents the angular average taken due to $\sum_{\theta'_{j_c}}$ in Eq.(4.52).

The left-hand side also becomes a 4×4 matrix due to the subband labeling

$$\sum_{j_c} \partial_t f_{j_c, \mathbf{k}} + i[H_{j_c, \mathbf{k}}, f_{j_c, \mathbf{k}}] + \frac{1}{2} \{ \nabla_{j_c, \mathbf{k}} H_{j_c, \mathbf{k}}, \nabla_{\mathbf{r}} f_{j_c, \mathbf{k}} \} - \frac{1}{2} \{ \nabla_{\mathbf{r}} H_{\mathbf{r}}, \nabla_{j_c, \mathbf{k}} f_{j_c, \mathbf{k}} \} = I_{\mathbf{k}}. \quad (4.58)$$

[†]We have also used Eq.(3.34) to write it in terms of the f distribution.

As in section 4.2 one needs to perform the distribution function expansion. For the two subbands case we do it accordingly $f_{j,\mathbf{k}} = g_{j,\mathbf{k}}^i \sigma_i$ and $\langle f_{j,\mathbf{k}} \rangle = \langle g_{j,\mathbf{k}}^i \rangle \sigma_i$. Therefore, what was once a 4x4 matrix, for two subbands becomes a 8x8 matrix. The left-hand side it's a huge matrix and we won't display it here but the final result. The same approximations and Fourier transforms used to find the 4x4 \mathcal{K} in Eq.(4.24) are also used to determine the 8x8 matrix, however this time carrying the subband band index label. What follows next are very similar steps as in Eqs. (4.26) to (4.28)

$$\tau_0 \mathcal{K}_{j_c} \mathbf{g}_{j,\mathbf{k}} = \sum_{j_c} \left[-\mathbf{g}_{j,\mathbf{k}} + \langle \mathbf{g}_{j_c,\mathbf{k}} \rangle \right] P_{j,j_c},$$

$$\sum_{j_c} [\tau_0 \mathcal{K}_{j_c} + \mathcal{I}_{8 \times 8} P_{j,j_c}] \mathbf{g}_{j,\mathbf{k}} = \sum_{j_c} \langle \mathbf{g}_{j_c,\mathbf{k}} \rangle P_{j,j_c}, \quad (4.59)$$

$$\mathbf{g}_{j,\mathbf{k}} = \sum_{j_c} [\tau_0 \mathcal{K}_{j_c} + \mathcal{I}_{8 \times 8} P_{j,j_c}]^{-1} \langle \mathbf{g}_{j_c,\mathbf{k}} \rangle P_{j,j_c}, \quad (4.60)$$

where the vectors are $\mathbf{g}_{j,\mathbf{k}} = [g_{1,\mathbf{k}}^0, g_{1,\mathbf{k}}^x, g_{1,\mathbf{k}}^y, g_{1,\mathbf{k}}^z, g_{2,\mathbf{k}}^0, g_{2,\mathbf{k}}^x, g_{2,\mathbf{k}}^y, g_{2,\mathbf{k}}^z]^T$ and $\langle \mathbf{g}_{j_c,\mathbf{k}} \rangle = \left[\langle g_{1,\mathbf{k}}^0 \rangle, \langle g_{1,\mathbf{k}}^x \rangle, \langle g_{1,\mathbf{k}}^y \rangle, \langle g_{1,\mathbf{k}}^z \rangle, \langle g_{2,\mathbf{k}}^0 \rangle, \langle g_{2,\mathbf{k}}^x \rangle, \langle g_{2,\mathbf{k}}^y \rangle, \langle g_{2,\mathbf{k}}^z \rangle \right]^T$. The T stands for transpose and 1, 2 for the subbands.

From the last section we've seen it that one is able to close Eq.4.60 by taking the angular average in the left-hand side. Therefore,

$$\langle \mathbf{g}_{j,\mathbf{k}} \rangle = \sum_{j_c} \left\langle [\tau_0 \mathcal{K}_{j_c} + \mathcal{I}_{8 \times 8} P_{j,j_c}]^{-1} \right\rangle \langle \mathbf{g}_{j_c,\mathbf{k}} \rangle P_{j,j_c}. \quad (4.61)$$

The procedure to find the the drift-diffusion for two subbands is the same as for the 4x4 drift-diffusion matrix in section 4.2. One has to Fourier transform back the variable ω inside \mathcal{K}_{j_c} to t and define the drift-diffusion equation as

The two subbands diffusion equation is

$$\frac{\partial}{\partial t} \begin{pmatrix} N_1(\mathbf{q}, t) \\ \vec{S}_1(\mathbf{q}, t) \\ N_2(\mathbf{q}, t) \\ \vec{S}_2(\mathbf{q}, t) \end{pmatrix} = - \begin{pmatrix} \mathcal{D}_1(\mathbf{q}) + \gamma_1 \mathcal{I}_4 & \frac{P_{12}}{P_{11}} \mathcal{D}_1(\mathbf{q}) - \gamma_1 \mathcal{I}_4 \\ \frac{P_{21}}{P_{22}} \mathcal{D}_2(\mathbf{q}) - \gamma_2 \mathcal{I}_4 & \mathcal{D}_2(\mathbf{q}) + \gamma_2 \mathcal{I}_4 \end{pmatrix} \begin{pmatrix} N_1(\mathbf{q}, t) \\ \vec{S}_1(\mathbf{q}, t) \\ N_2(\mathbf{q}, t) \\ \vec{S}_2(\mathbf{q}, t) \end{pmatrix}, \quad (4.62)$$

where the 8-vectors $[N_1, \vec{S}_1, N_2, \vec{S}_2]^T = [N_1, S_{1x}, S_{1y}, S_{1z}, N_2, S_{2x}, S_{2y}, S_{2z}]^T$ are written in a compact notation, and \mathcal{I}_4 is a 4×4 identity matrix. The diffusion matrix $\mathcal{D}_j(\mathbf{q})$ for each subband j is

$$\mathcal{D}_j(\mathbf{q}) = \begin{pmatrix} D_j q^2 & -i\theta_{SH}^{(xj)} D_j q_{j1} q_y & -i\theta_{SH}^{(yj)} D_j q_{j2} q_x & 0 \\ -i\theta_{SH}^{(xj)} D_j q_{j1} q_y & D_j q^2 + \frac{1}{\tau_{xj}} & 0 & 2iD_j q_{j1} q_x \\ -i\theta_{SH}^{(yj)} D_j q_{j2} q_x & 0 & D_j q^2 + \frac{1}{\tau_{yj}} & -2iD_j q_{j2} q_y \\ 0 & -2iD_j q_{j1} q_x & 2iD_j q_{j2} q_y & D_j q^2 + \frac{1}{\tau_{xj}} + \frac{1}{\tau_{yj}} \end{pmatrix}. \quad (4.63)$$

The elements on these matrices are

$$D_j = \frac{1}{(P_{j1} + P_{j2})} \frac{\tau_0 k_{Fj}^2}{2m^2}, \quad (4.64)$$

$$\gamma_j = \frac{P_{12}(P_{j1} + P_{j2})}{P_{jj}\tau_0}, \quad (4.65)$$

$$q_{j1} = 2m\lambda_{j1} = 2m(\beta_j + \alpha_j), \quad (4.66)$$

$$q_{j2} = 2m\lambda_{j2} = 2m(\beta_j - \alpha_j), \quad (4.67)$$

$$\theta_{SH}^{(xj)} = -\frac{q_{j2}/q_{j1}}{2mD_j} + \frac{q_{j1}q_{j2}\tau_0}{2m(P_{j1} + P_{j2})}, \quad (4.68)$$

$$\theta_{SH}^{(yj)} = -\frac{q_{j1}/q_{j2}}{2mD_j} + \frac{q_{j1}q_{j2}\tau_0}{2m(P_{j1} + P_{j2})}, \quad (4.69)$$

$$\frac{1}{\tau_{xj}} = D_j q_{j1}^2, \quad (4.70)$$

$$\frac{1}{\tau_{yj}} = D_j q_{j2}^2. \quad (4.71)$$

Here D_j is the diffusion constant for each subband j , θ_{SH} is the spin Hall angle (SHEN; RAIMONDI; VIGNALE, 2014) that couples the charge and spin subspaces for each subband j , q_{j1} and q_{j2} are the spin-orbit intensities written in units of momentum, and γ_j are subband relaxation rates.

Notice that some terms on Eq.(4.62) are novel and have not yet been discussed in the literature. However, due to the complexity of this 8×8 matrix equation, we do not have yet proper interpretation for the effect of all terms on the spin-charge dynamics. To accomplish this, further systematic numerical analysis is required, which will be developed in a future publication. To obtain Eq. (4.62) we have followed approximations equivalent to those in the single subband regime.

4.5. Crossed PSH regime

To illustrate the results of the spin dynamics with two subbands, we consider the crossed PSH (cPSH) regime (FU et al., 2016) (FERREIRA et al., 2017). There, the first subband is set on the PSH regime with $\alpha_1 = +\beta_1$, while the second subband is set on a

Table 4 – Parameters for the two subbands PSH model on the crossed PSH regime [citar Gerson/PRB] with $\alpha_1 = \beta_1$ and $\alpha_2 = -\beta_2$. The values of $\beta_1 = \beta_2$ range from the a typical 0.37 meV nm to an exaggerated 5.0 meV nm.

Parameter	Value	Description
m	$0.067m_0$	Effective mass (GaAs)
n_s	$8 \times 10^{11} \text{ cm}^{-2}$	2DEG density
$\varepsilon_2 - \varepsilon_1$	7 meV	Subband energy splitting
(n_1, n_2)	$(5.0, 3.0) \times 10^{11} \text{ cm}^{-2}$	Density per subband
$\beta_1 = \beta_2$	0.37 – 5.0 meV nm	Linear Dresselhaus for each subband
τ_0	1 ps	Momentum scattering time

transverse PSH regime with $\alpha_2 = -\beta_2$ [see spin textures in k -space in Figure 8(c)]. The full set of parameters considered here are shown in Table 4, which were extracted from Ref.(FERREIRA et al., 2017). This table shows two possible values for the spin-orbit intensity (0.37 and 5.0 meV nm). The first is a typical value for GaAs quantum wells, while the second is an exaggeratedly large value that we choose to illustrate the effects of the SOC intensity on the spin dynamics.

When the subbands are set on the cPSH regime with orthogonal uniaxial spin textures ($\alpha_1 = \beta_1$ for the first subband, and $\alpha_2 = -\beta_2$ for the second), scattering from one subband to the other require a spin rotation that cannot be induced by scalar impurities. Therefore, a recent heuristic derivation of the spin drift-diffusion equation have assumed that the subbands are uncoupled in this regime (FU et al., 2016). In contrast, the random walk model of Ref. (FERREIRA et al., 2017) considers two possible regimes for the intersubband coupling.

Indeed, we find here that, depending on the SOC intensity, the spin dynamics follow either a weak or strong intersubband coupling regime. To classify these regimes, notice that the SOC splits each subband further into spin “sub”-subbands, as shown in Figure 8. This spin-splitting can be roughly estimated by the SOC energy $E_{SOC}^{(j)} \approx \beta_j k_F^{(j)}$ for each subband. Complementary, the impurity scattering induces a energy broadening of $\Gamma_S \approx \hbar/\tau_0$. Therefore, if $E_{SOC}^{(j)} \ll \Gamma_S$, the spin “sub”-subbands on each subband j are effectively degenerate. Consequently, the spin-polarization of each subband shown in Figure 8 vanishes, and the scattering between subbands is allowed, redering what we call a **strong intersubband coupling regime**. On the other hand, if $E_{SOC}^{(j)} \gg \Gamma_S$ intersubband scattering is forbidden, as discussed above, due to the crossed spin polarization shown in Figure 8. In this case we find a **weak intersubband coupling regime**.

Figure 11 shows the spin dynamics in the strong coupling regime. The spin pattern in both subbands are nearly identical, apart from small differences due to their different

diffusion constant. The overall pattern is nearly circular, which matches the heuristic result found with a random walk model in Ref. (FERREIRA et al., 2017). There, the spin dynamics on the strong coupling regime is approximately equivalent to that of a single effective subband with average $\alpha_{eff} = (\alpha_1 + \alpha_2)/2 = 0$ and $\beta_{eff} = (\beta_1 + \beta_2)/2 = \beta_1 = \beta_2$. Since $\alpha_{eff} = 0$, this effective subband has Dresselhaus type of spin texture in k -space, as in Figure 8. Consequently it does not match a uniaxial spin pattern and the spin diffusion is nearly isotropic, hence the circular pattern of Fig. 11. In contrast, Fig. 12 shows the spin diffusion in the weak coupling regime. In this case the subbands are nearly independent. Indeed, the spin diffusion of the first subband shows horizontal stripes due to the uniaxial PSH regime given by $\alpha_1 = +\beta_1$, while the second subband shows vertical stripes due to the orthogonal regime $\alpha_2 = -\beta_2$. However, since the diffusion constant of the first and second subbands are different, the total spin map follows the pattern of the subband that shows a slower relaxation. If the diffusion and relaxation rates of both subbands were equal, the total spin would show the chessboard pattern discussed in Refs. (FU et al., 2016), (FERREIRA et al., 2017). However, this regime can only occur for large SOC, such that $E_{SOC}^{(j)} \gg \Gamma_S$, which might not be achievable in real samples.

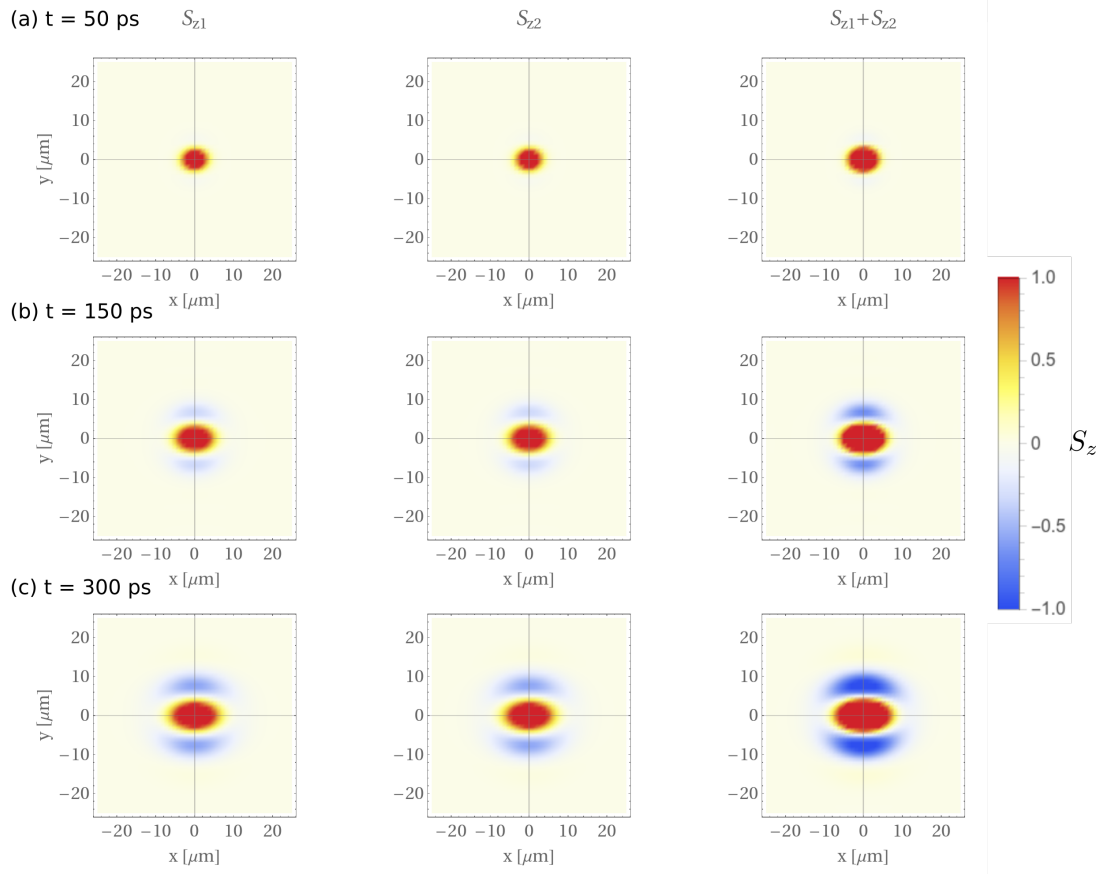


Figure 11 – Spin diffusion for the first (left), second (center) subband and total spin density at different times t . Here the parameters follow Table 4 with $\beta_1 = \beta_2 = 0.37$ meV nm. Since the SOC is small, it shows the strong intersubband coupling regime. The color code indicates the local spin z-component with the intensity saturated for better visualization. The overall intensity falls approximately as $\sim e^{-t/\tau_s}$, with a relaxation time of $\tau_S \sim 50$ ps, extracted from the numerical results.

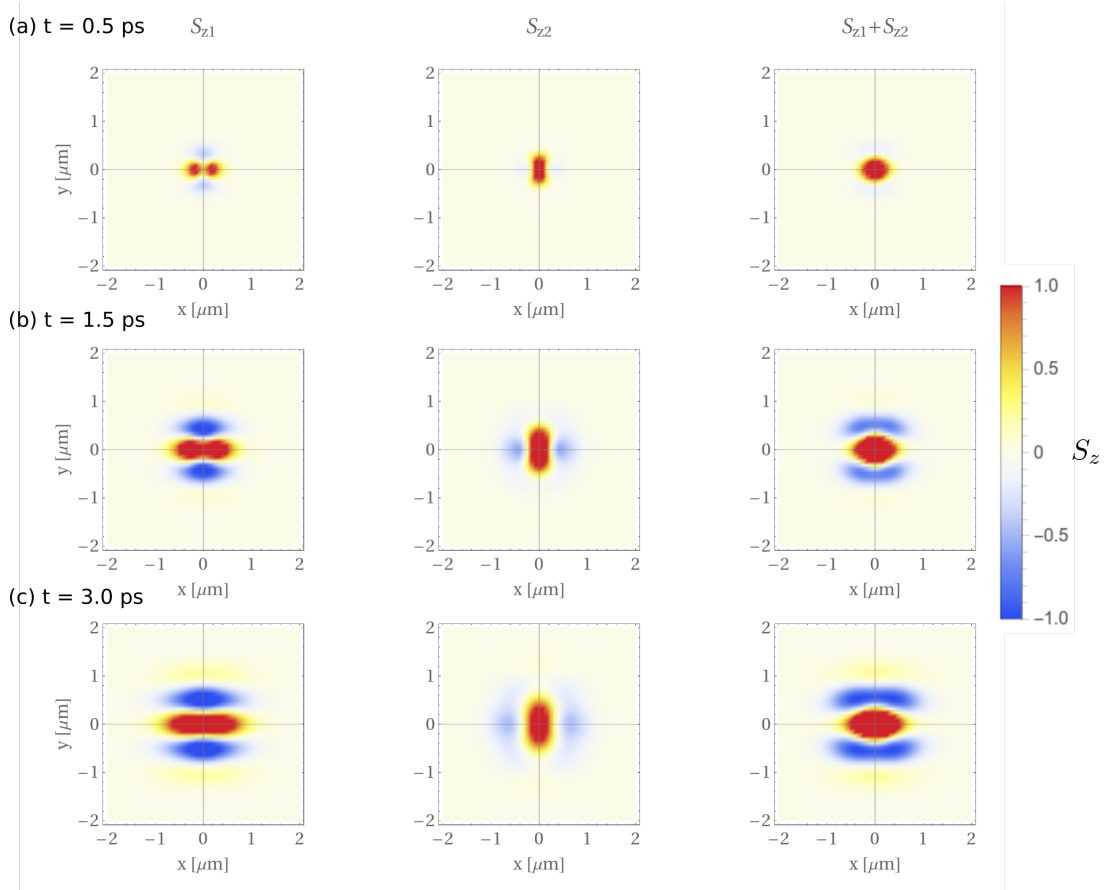


Figure 12 – Spin diffusion for the first (left), second (center) subband and total spin density at different times t . Here the parameters follow Table 4 with $\beta_1 = \beta_2 = 5.0$ meV nm. Since the SOC is large, it shows the weak intersubband coupling regime. As in Fig. 11, the color code is saturated, and the overall intensity falls as $\sim e^{-t/\tau_s}$, with $\tau_s \sim 1$ ps.

5 Conclusions

In this dissertation we have aimed to learn the non-equilibrium Greens function formalism, a complex however necessary approach for the spin drift-diffusion, which is an essential topic linked to our research field of interest, spintronics. Asking how the electron distribution function $f_{\mathbf{k}}$ changes over time in a system out of equilibrium, i.e., determining the Boltzmann transport equation (BTE), requires a challenging formalism. One has to use Greens functions, and luckily, the Dyson equation is able to account all the possible interactions. However, propagators are not enough to derive the BTE and one is compelled to use further mathematical tools, such as the Keldysh formalism and appropriate approximations.

The Keldysh formalism is based on the equivalence of the quantum mechanic time evolution operator to an abstract contour as in Figure 3. It enables a infinity string of operators to be broken down into pairs, turning impossible equations to manageable ones. Then, one is able to build the Keldysh space, a cornerstone of our work. The very fascinating characteristic of the propagators given by the Keldysh space, is that they still keep the statistical essence of the Dyson equation, enabling one to construct a non-equilibrium Dyson equation in the Keldysh space. Therefore, also yielding the kinetic equations.

Mastering the formalism really paid off when including spin in the BTE and deriving the spin drift-diffusion equation. With systematic derivations, we have been able to solve it for the persistent spin helix (PSH) regime forming the beautiful pattern shown in Figure 9. If the Keldysh formalism wasnt a challenged enough, weve also been able to extend the PSH towards novel system: a formal derivation of the spin drift-diffusion equation for two subbands. The derivation process follows straightforward from the single subband case, except we now have a 8×8 matrix equation. We have found that the diffusion constant, as well as other dynamical paramters, are subband dependent and defined by an structural factor that depends on the geometry of the confining quantum well.

In view of a new result, theres yet much to be comprehend about it. Regardless, our result have shown different patterns for a weak and strong intersubband coupling regimes, corroborating the heuristic Random Walk model from Ref. (FERREIRA et al., 2017). We have found that these regimes are defined by the interplay between the spin-orbit energy splitting, and the energy broadening induced by the impurity scattering.

We have used approximations such as the quasi-particle and the low impurity limit. To avoid complications we had to assume that spin-orbit interaction and subband correlations in the spectral function were negligible. Eventually, these approximations will have to be revised in order to build a more general equation that accounts for subbands

crossings. Despite of that, the obtained equations already shine a light into the spin relaxation time for the two subbands problem.

The next steps of our research are a meticulous numerical analysis of our equations for two subbands, since the complexity of the 8×8 matrix equation does not seem to hold useful analytical solutions. Particularly, our next goal is comprehend how the spin relaxation time depends on the spin-orbit couplings and structural factors for weak and strong intersubband coupling regime. Together with the results already presented in this dissertation, this complement shall be soon submitted for publication. Additionally, these analysis can be compared to recent experimental (unpublished) results obtained by our collaborators.

As future perspectives, we intend to turn our attention to the spin diffusion in topological insulators and crossings of Landau levels on GaAs quantum wells. The strong spin-orbit coupling of topological insulators shall yield non-trivial bulk diffusive dynamics, while its topological edge states might add yet another degree-of-freedom for the dynamics. The diffusive dynamics on Landau level crossings is yet unexplored, and its interplay with the spin-orbit couplings and electron-electron interactions is complex and interesting topic that can be investigated with the formalism developed here.

In conclusion, the developments shown in this dissertation have given us a formal and powerful tool to tackle a variety of distinct problems in condensed matter and, particularly, spintronics. Thus, mastering the Keldysh and non-equilibrium Greens function formalism will certainly enrich our future developments, allowing us to investigate novel problems, even beyond the spin drift-diffusion ones that are presented here.

Bibliography

- BERNEVIG, B. A.; ORENSTEIN, J.; ZHANG, S.-C. Exact $su(2)$ symmetry and persistent spin helix in a spin-orbit coupled system. *Phys. Rev. Lett.*, American Physical Society, v. 97, p. 236601, Dec 2006. Disponível em: <<https://link.aps.org/doi/10.1103/PhysRevLett.97.236601>>.
- BRUUS, H.; FLENSBERG, K. *Many-body quantum theory in condensed matter physics: an introduction*. New York: Oxford university press, 2004.
- DANIELEWICZ, P. Quantum theory of nonequilibrium processes, i. *Annals of Physics*, v. 152, p. 239–304, 1984.
- DATTA, S.; DAS, B. Electronic analog of the electrooptic modulator. *Applied Physics Letters*, v. 56, n. 7, p. 665–667, 1990. Disponível em: <<https://doi.org/10.1063/1.102730>>.
- DIENY, B. et al. Giant magnetoresistive in soft ferromagnetic multilayers. *Phys. Rev. B*, American Physical Society, v. 43, p. 1297–1300, Jan 1991. Disponível em: <<https://link.aps.org/doi/10.1103/PhysRevB.43.1297>>.
- DRESSELHAUS, G. Spin-orbit coupling effects in zinc blende structures. *Phys. Rev.*, American Physical Society, v. 100, p. 580–586, Oct 1955. Disponível em: <<https://link.aps.org/doi/10.1103/PhysRev.100.580>>.
- FERREIRA, G. J. et al. Spin drift and diffusion in one- and two-subband helical systems. *Phys. Rev. B*, American Physical Society, v. 95, p. 125119, Mar 2017. Disponível em: <<https://link.aps.org/doi/10.1103/PhysRevB.95.125119>>.
- FERT, A. Nobel lecture: Origin, development, and future of spintronics. *Rev. Mod. Phys.*, American Physical Society, v. 80, p. 1517–1530, Dec 2008. Disponível em: <<https://link.aps.org/doi/10.1103/RevModPhys.80.1517>>.
- FU, J. et al. Persistent skyrmion lattice of noninteracting electrons with spin-orbit coupling. *Phys. Rev. Lett.*, American Physical Society, v. 117, p. 226401, Nov 2016. Disponível em: <<https://link.aps.org/doi/10.1103/PhysRevLett.117.226401>>.
- GRÜNBERG, P. A. Nobel lecture: From spin waves to giant magnetoresistance and beyond. *Rev. Mod. Phys.*, American Physical Society, v. 80, p. 1531–1540, Dec 2008. Disponível em: <<https://link.aps.org/doi/10.1103/RevModPhys.80.1531>>.
- HAUG, H.; JAUHO, A.-P. *Quantum kinetics in transport and optics of semiconductors*. New York: Springer, 2008. v. 2.
- HUANG, K. *Statistical mechanics*. New York: John Wiley & Sons, 1987.
- KADANOFF, L. P. *Quantum statistical mechanics*. Boca Raton: CRC Press, 2018.
- KAISER, D. Physics and Feynman's Diagrams: In the hands of a postwar generation, a tool intended to lead quantum electrodynamics out of a decades-long morass helped transform physics. *American Scientist*, v. 93, n. 2, p. 156–165, 2005.

KELDYSH, L. V. Diagram technique for nonequilibrium processes. *Zh. Eksp. Teor. Fiz.*, v. 47, p. 1018, 1964.

KOHDA, M.; SALIS, G. Physics and application of persistent spin helix state in semiconductor heterostructures. *Semiconductor Science and Technology*, IOP Publishing, v. 32, n. 7, p. 073002, jun 2017. Disponível em: <<https://doi.org/10.1088%2F1361-6641%2Faa5dd6>>.

LARKIN, A.; OVCHINNIKOV, Y. Nonlinear conductivity of superconductors in the mixed state. *Sov. Phys. JETP*, v. 41, n. 5, p. 960–965, 1975.

LIU, X.; SINOVA, J. Unified theory of spin dynamics in a two-dimensional electron gas with arbitrary spin-orbit coupling strength at finite temperature. *Phys. Rev. B*, American Physical Society, v. 86, p. 174301, Nov 2012. Disponível em: <<https://link.aps.org/doi/10.1103/PhysRevB.86.174301>>.

MACHADO, K. D. *Teoria do eletromagnetismo*. Ponta Grossa: UEPG, 2007.

MACIEJKO, J. An introduction to nonequilibrium many-body theory. *Lecture Notes*, Springer, 2007.

MATTUCK, R. D. *A guide to Feynman diagrams in the many-body problem*. New York: Dover publications, 1992.

ODASHIMA, M. M.; PRADO, B. G.; VERNEK, E. Pedagogical introduction to equilibrium Green's functions: condensed-matter examples with numerical implementations. *Revista Brasileira de Ensino de Física*, scielo, v. 39, 00 2017. ISSN 1806-1117. Disponível em: <http://www.scielo.br/scielo.php?script=sci_arttext&pid=S1806-11172017000100402&nrm=iso>.

PATHRIA, R.; BEALE, P. *Statistical Mechanics*. Oxford: Butterworth-Heinemann, 2011.

RAIMONDI, R.; SCHWAB, P. Interplay of intrinsic and extrinsic mechanisms to the spin Hall effect in a two-dimensional electron gas. *Physica E*, v. 42, n. 4, p. 952–955, 2010. Disponível em: <<http://www.sciencedirect.com/science/article/pii/S1386947709004111>>.

RAIMONDI, R. et al. Spin-orbit interaction in a two-dimensional electron gas: A su(2) formulation. *Annalen der Physik*, v. 524, n. 34. Disponível em: <<https://onlinelibrary.wiley.com/doi/abs/10.1002/andp.201100253>>.

RAMMER, J. *Quantum field theory of non-equilibrium states*. New York: Cambridge University Press, 2007.

RAMMER, J. *Quantum transport theory*. Boca Raton: CRC Press, 2018.

RAMMER, J.; SMITH, H. Quantum field-theoretical methods in transport theory of metals. *Rev. Mod. Phys.*, American Physical Society, v. 58, p. 323–359, Apr 1986. Disponível em: <<https://link.aps.org/doi/10.1103/RevModPhys.58.323>>.

RASHBA, E. I. Properties of semiconductors with an extremum loop. I. Cyclotron and combinational resonance in a magnetic field perpendicular to the plane of the loop. *Sov. Phys. Solid. State*, v. 2, p. 1109–1122, 1960.

RICHMOND, P.; MIMKES, J.; HUTZLER, S. *Econophysics and physical economics*. New York: Oxford University Press, 2013.

SCHLIEMANN, J.; EGUES, J. C.; LOSS, D. Nonballistic spin-field-effect transistor. *Phys. Rev. Lett.*, American Physical Society, v. 90, p. 146801, Apr 2003. Disponível em: <<https://link.aps.org/doi/10.1103/PhysRevLett.90.146801>>.

SHEN, K.; RAIMONDI, R.; VIGNALE, G. Theory of coupled spin-charge transport due to spin-orbit interaction in inhomogeneous two-dimensional electron liquids. *Phys. Rev. B*, American Physical Society, v. 90, p. 245302, Dec 2014. Disponível em: <<https://link.aps.org/doi/10.1103/PhysRevB.90.245302>>.

Appendix

APPENDIX A – Boltzmann weighting factor

The relation between the time evolution operator in the interaction picture between Heisenberg's is give by

$$U_I(t, t_0) = e^{iH_0(t-t_0)}U_{\mathcal{H}}(t, t_0), \quad (\text{A.1})$$

known as the Dyson formula. Let the Hamiltonian be composed of three terms $H = H_0 + V(t)$, where H_0 is free Hamiltonian and $V(t)$ is a time dependent interaction. The time evolution operators are then given by

$$T \exp\left\{-i \int_{t_0}^t V_I(t'') dt''\right\} = e^{iH_0(t-t_0)} e^{iH(t-t_0)} \quad (\text{A.2})$$

Taking the complex time limit t_0 to $t_0 - i\beta$

$$T \exp\left\{-i \int_{t_0}^{t_0-i\beta} + V_I(t'') dt''\right\} = e^{\beta H_0} e^{-\beta H} \quad (\text{A.3})$$

The exponentials carry operators, so one must be careful handling it. We work from the left by multiplying $e^{-\beta H_0}$

$$e^{-\beta H'} = e^{-\beta H_0} T\left(\exp\left\{-i \int_{t_0}^{t_0-i\beta} V_I(t'') dt''\right\}\right) \quad (\text{A.4})$$

This is a very important result, it enables us to re-write the average Green's functions which eventually will allow us to use the Wick's theorem.

APPENDIX B – Operators using closed contour

In this Appendix we verify the equivalence of the time evolution operator in Eq.2.60 to that Eq.2.62. We start by expanding the exponential in Eq.2.62 to the n th

$$\hat{O}_{\mathcal{H}}(t) = \sum_{n=0}^{\infty} \frac{(-i)^n}{n!} \int_C d\tau_1 \cdots \int_C d\tau_n T_c(V_I(\tau_1) \dots V_I(\tau_n)) \hat{O}_I(t) \quad (\text{B.1})$$

The trick correspond to split the contour into two parts, $c = \vec{c} + \overleftarrow{c}$. We denote \vec{c} and \overleftarrow{c} by the forward and backward contour, respectively(note, we are NOT separating the contour in half necessarily, as will become clear soon enough). Now we consider that in the forward contour we have m terms (m contour variables), consequently the backward part has $n - m$ terms. So we ask ourselves, how many subsets of m terms can one take out of the total number of terms ? We can answer this question by calculating all combinations $\frac{n!}{m!(n-m)!}$, thus we write the integral part

$$\begin{aligned} \int_C d\tau_1 \cdots \int_C d\tau_n T_c(V_I(\tau_1) \dots V_I(\tau_n)) \hat{O}_I(t) &= \sum_{m=0}^n \frac{n!}{m!(n-m)!} \\ &\times \int_{\overleftarrow{c}} d\tau_{m+1} \cdots \int_{\overleftarrow{c}} d\tau_n T_{\overleftarrow{c}}(V_I(\tau_{m+1}) \dots V_I(\tau_n)) \hat{O}_I(t) \\ &\times \int_{\vec{c}} d\tau_1 \cdots \int_{\vec{c}} d\tau_m T_{\vec{c}}(V_I(\tau_1) \dots V_I(\tau_m)) \end{aligned} \quad (\text{B.2})$$

Although the equation above looks difficult, it shows exactly what we mean by calculating the combinations, say we choose $m = 0$, that means we're not taking any terms from the forward contour, we are not splitting it and we have B.1 back again. Say we chose $m = 1$

$$\begin{aligned} \int_C d\tau_1 \cdots \int_C d\tau_n T_c(V_I(\tau_1) \dots V_I(\tau_n)) \hat{O}_I(t) &= \sum_{m=0}^n \frac{n!}{(n-1)!} \\ &\times \int_{\overleftarrow{c}} d\tau_2 \cdots \int_{\overleftarrow{c}} d\tau_n T_{\overleftarrow{c}}(V_I(\tau_2) \dots V_I(\tau_n)) \hat{O}_I(t) \int_{\vec{c}} d\tau_1 T_{\vec{c}} V_I(\tau_1) \end{aligned} \quad (\text{B.3})$$

therefore, we've split the contour into 1 term as the forward and $n - 1$ as the backward contours.

To proceed with our analyses, we split the sum into a product of two sums compensated by a Kronecker function, but before using it, we show why this can be done.

Consider the sum

$$\sum_i^n x_i y_i = x_1 y_1 + x_2 y_2 + \dots x_n y_n. \quad (\text{B.4})$$

Now consider the product of two sums

$$\begin{aligned} \sum_i^\infty x_i \sum_j^\infty y_j &= (x_1 + x_2 + \dots) \sum_j^n y_j = \\ &= (x_1 + x_2 + \dots x_n)(y_1 + y_2 + \dots y_n) = x_1 y_1 + x_1 y_2 + \dots \end{aligned} \quad (\text{B.5})$$

This is obviously not the same sum as the first one, unless, we make it to be, by inserting a Kronecker functions $\delta_{i,j}$, so all terms like $x_1 y_2$ are zero. Hence we split the sum in equation B.4

$$\begin{aligned} \int_C d\tau_1 \cdots \int_C d\tau_n T_c(V_I(\tau_1) \dots V_I(\tau_n)) \hat{O}_I(t) &= \sum_k^\infty \sum_m^\infty \frac{n!}{m!k!} \delta_{n,k+m} \\ &\times \int_{\overleftarrow{c}} d\tau_1 \cdots \int_{\overleftarrow{c}} d\tau_k T_{\overleftarrow{c}}(V_I(\tau_1) \dots V_I(\tau_k)) \hat{O}_I(t) \\ &\times \int_{\overrightarrow{c}} d\tau_1 \cdots \int_{\overrightarrow{c}} d\tau_m T_{\overrightarrow{c}}(V_I(\tau_1) \dots V_I(\tau_m)). \end{aligned} \quad (\text{B.6})$$

Replacing it on B.1 we get

$$\begin{aligned} \hat{O}_{\mathcal{H}}(t) &= \sum_k^\infty \sum_m^\infty \frac{(-i)^k (-i)^m}{m!k!} \\ &\times \int_{\overleftarrow{c}} d\tau_1 \cdots \int_{\overleftarrow{c}} d\tau_k T_{\overleftarrow{c}}(V_I(\tau_1) \dots V_I(\tau_k)) \hat{O}_I(t) \\ &\times \int_{\overrightarrow{c}} d\tau_1 \cdots \int_{\overrightarrow{c}} d\tau_m T_{\overrightarrow{c}}(V_I(\tau_1) \dots V_I(\tau_m)). \end{aligned} \quad (\text{B.7})$$

Recalling equations 2.62 and B.1

$$T_c\left(e^{\int_c d\tau V_I(\tau)} \hat{O}_I\right) = T_{\overleftarrow{c}}\left(e^{\int_{\overleftarrow{c}} d\tau V_I(\tau)}\right) \hat{O}_I(t) T_{\overrightarrow{c}}\left(e^{\int_{\overrightarrow{c}} d\tau V_I(\tau)}\right) \quad (\text{B.8})$$

We now parameterize the forward contour as $\tau = t'$ with $t_0 < t' < t$ yielding

$$T_{\overrightarrow{c}}\left(e^{-i \int_{\overrightarrow{c}} d\tau V_I(\tau)}\right) = T\left(e^{-i \int_{t_0}^t dt' V_I(t')}\right) = U_I(t, t_0) \quad (\text{B.9})$$

and we parameterize the backward contour such as $t < t' < t_0$

$$T_{\overleftarrow{c}}\left(e^{\int_{\overleftarrow{c}} d\tau V_I(\tau)}\right) = \tilde{T}\left(e^{\int_{t_0}^t dt' V_I(t')}\right) = U_I^\dagger(t, t_0) \quad (\text{B.10})$$

therefore [B.8](#) becomes

$$T_c\left(e^{\int_e d\tau V_I(\tau)} \hat{O}_I\right) = U_I^\dagger(t, t_0) \hat{O}_I U_I(t, t_0) \quad (\text{B.11})$$

Comparing [Eq.B.11](#) to [Eq.2.57](#) we establish that [Eq.2.62](#) is indeed valid.

APPENDIX C – Wick's Theorem

The Wick's theorem states that we can break a string of field operators as sum of pairs, such that a general form wished can be written as

$$\langle T_c(c(\tau_N)c(\tau_{N-1})\cdots c(\tau_2)c(t_1)) \rangle = \sum_{a.p.p} \prod_{qq'} \langle T_c c_q(\tau) c_{q'}(\tau') \rangle \quad (\text{C.1})$$

c can be either a creation or annihilation operator

To determine if Eq.C.1 is true, consider the Hamiltonian for a bosonic system in equilibrium $H_b^0 \rightarrow H_b^0 - \mu_b N_b$ $\omega_q = \varepsilon_q - \mu_b$, the Hamiltonian

$$H_b^0 = \sum_q h_q = \sum_q \varepsilon_q a_q^\dagger a_q \quad (\text{C.2})$$

For one mode from the Hamiltonian one can notice

$$c_q h_q = (h_q - \lambda \omega_q) c_q \quad (\text{C.3})$$

$$\lambda = \begin{cases} +1 & c_q = a_q^\dagger \\ -1 & c_q = a_q \end{cases} \quad (\text{C.4})$$

$$c_q h_q^n = (h_q - \lambda \omega_q)^n c_q \quad (\text{C.5})$$

The statistical operator

$$\rho = \sum_q \rho_q \quad (\text{C.6})$$

$$\rho = \frac{e^{-\beta h_q}}{1 - e^{-\beta \omega_q}} = Z^{-1} e^{-\beta h_q} \quad (\text{C.7})$$

expanding the exponential in the equation above

$$c_q \rho = (e^{\beta \lambda \omega_q} - 1) \rho c_q \quad (\text{C.8})$$

taking the average of the commutator with an arbitrary operator \hat{A}

$$\langle [c_q, \hat{A}] \rangle = \text{tr}(\rho [c_q, \hat{A}]) \quad (\text{C.9})$$

employing the cyclist of the trace

$$\langle [c_q, \hat{A}] \rangle = -tr([c_q, \rho] \hat{A}) \quad (\text{C.10})$$

$$\langle [c_q, \hat{A}] \rangle = (1 - e^{\beta\lambda\omega_q}) tr(\rho c_q \hat{A}) \quad (\text{C.11})$$

$$\langle [c_q, \hat{A}] \rangle = (1 - e^{\beta\lambda\omega_q}) \langle c_q, \hat{A} \rangle \quad (\text{C.12})$$

If we also want to take into account fermions

$$\langle [c_q, \hat{A}]_\gamma \rangle = (1 + \gamma e^{\beta\lambda\omega_q}) \langle c_q, \hat{A} \rangle \quad (\text{C.13})$$

$\gamma = \mp 1$ for bose and fermi statistics respectively

Consider a string of $2N$ field operators

$$S_N = \langle T_c(c(\tau_{2N})c(\tau_{2N-1}) \cdots c(\tau_2)c(t_1)) \rangle \quad (\text{C.14})$$

In equation above the product of field operator are already under time ordering

$$S_N = \left\langle \prod_{n=1}^{2N} c(\tau_n) \right\rangle = \left\langle c(\tau_{2N}) \prod_{n=1}^{2N-1} c(\tau_n) \right\rangle \quad (\text{C.15})$$

Using equation (C.13)

$$S_N = (1 - 1e^{\beta\lambda\omega_q})^{-1} \left\langle \left[c(\tau_{2N}), \prod_{n=1}^{2N-1} c(\tau_n) \right] \right\rangle \quad (\text{C.16})$$

the commutator

$$\left[c(\tau_{2N}), \prod_{n=1}^{2N-1} c(\tau_n) \right] = \left[c(\tau_{2N}), c(\tau_{2N-1})c(\tau_{2N-2})c(\tau_{2N-3}) \prod_{n=1}^{2N-4} c(\tau_n) \right] \quad (\text{C.17})$$

using the properties of the commutator

$$\begin{aligned}
\left[c(\tau_{2N}), \prod_{n=1}^{2N-1} c(\tau_n) \right] &= \left[c(\tau_{2N}), c(\tau_{2N-1}) \right] \prod_{n=1}^{2N-1} c(\tau_n) \\
&+ c(\tau_{2N-1}) \left[c(\tau_{2N}), c(\tau_{2N-2}) \right] \prod_{n=1}^{2N-3} c(\tau_n) \\
&+ c(\tau_{2N-1})c(\tau_{2N-2}) \left[c(\tau_{2N}), c(\tau_{2N-3}) \right] \prod_{n=1}^{2N-4} c(\tau_n) \\
&+ c(\tau_{2N-1})c(\tau_{2N-2})c(\tau_{2N-3}) \left[c(\tau_{2N}), \prod_{n=1}^{2N-4} c(\tau_n) \right] \quad (C.18)
\end{aligned}$$

if we keep expanding the commutator in the last term eventually we would get an equation like

$$\left\langle \left[c(\tau_{2N}), \prod_{n=1}^{2N-1} c(\tau_n) \right] \right\rangle = \left\langle \sum_{n=1}^{2N-1} \left[c(\tau_{2N}), c(\tau_n) \right] \right\rangle \left\langle \prod_{n \neq n'=1}^{2N-1} c(\tau_{n'}) \right\rangle \quad (C.19)$$

which according (C.16) is written

$$\left\langle \left[c(\tau_{2N}), \prod_{n=1}^{2N-1} c(\tau_n) \right] \right\rangle = (1 - e^{\beta\lambda\omega_q}) \left\langle \sum_{n=1}^{2N-1} c(\tau_{2N})c(\tau_n) \right\rangle \left\langle \prod_{n \neq n'=1}^{2N-1} c(\tau_{n'}) \right\rangle \quad (C.20)$$

Adding back the contour ordering operator to ensure that the field operators will be correctly placed

$$S_N = \sum_{n=1}^{2N-1} \left\langle T_c c(\tau_{2N})c(\tau_n) \right\rangle \left\langle T_c \left(\prod_{n \neq n'=1}^{2N-1} c(\tau_{n'}) \right) \right\rangle \quad (C.21)$$

Equation (C.21) has the same form as (C.1), thus is true that for a system in equilibrium evolving with a free Hamiltonian can be broken into a sum of all possible pairs. For the case of Fermions is the same analyses, except we have to use the property $[A, BC] = \{B, A\}C - B\{C, A\}$.

APPENDIX D – Convolution relation in the Wigner coordinates

A very important step to derive the Quantum Boltzmann equation is the Gradient expansion. It consists in expanding the convolution integrals into exponential functions with derivatives regard the Wigner coordinates.

Consider the convolution C

$$C(\mathbf{r}_1, t_1, \mathbf{r}_2, t_2) = \int dt' \int d\mathbf{r}' A(\mathbf{r}_1, t_1, \mathbf{r}', t') B(\mathbf{r}', t', \mathbf{r}_2, t_2), \quad (\text{D.1})$$

the Wigner coordinates

$$\mathbf{R} = \frac{\mathbf{r}_1 + \mathbf{r}_2}{2} \quad \mathbf{r} = \mathbf{r}_1 - \mathbf{r}_2, \quad (\text{D.2})$$

$$T = \frac{t_1 + t_2}{2} \quad t = t_1 - t_2, \quad (\text{D.3})$$

are written so that

$$C(\mathbf{r}_1, t_1, \mathbf{r}_2, t_2) \rightarrow C(\mathbf{r}, t, \mathbf{R}, T). \quad (\text{D.4})$$

The Wigner coordinates introduce four new variables, the fast variables (\mathbf{r}, t) and the slow variables with respect to the center of mass (\mathbf{R}, T) which will be used for the gradient expansion.

The tricky part and purely mathematical, is a change of variables that seems completely arbitrary, however yielding the desired result ([MACIEJKO, 2007](#)). First for A

- $\mathbf{r}_1 \rightarrow \mathbf{r}_1 - \mathbf{r}', \quad t_1 \rightarrow t_1 - t'.$
- $\mathbf{r}' \rightarrow \frac{1}{2}(\mathbf{r}_1 + \mathbf{r}'), \quad t' \rightarrow \frac{1}{2}(t_1 + t').$

For B

- $\mathbf{r}' \rightarrow \mathbf{r}' - \mathbf{r}_2, \quad t' \rightarrow t' - t_2.$
- $\mathbf{r}_2 \rightarrow \frac{1}{2}(\mathbf{r}' + \mathbf{r}_2), \quad t_2 \rightarrow \frac{1}{2}(t' + t_2).$

Therefore, $A(\mathbf{r}_1 - \mathbf{r}', t_1 - t', \frac{1}{2}(\mathbf{r}_1 + \mathbf{r}'), \frac{1}{2}(t_1 + t'))$ and $B(\mathbf{r}' - \mathbf{r}_2, t' - t_2, \frac{1}{2}(\mathbf{r}' + \mathbf{r}_2), \frac{1}{2}(t' + t_2))$. Using the Wigner coordinates we write A and B as

$$A(\mathbf{r}_1, t_1, \mathbf{r}', t') = A\left(\mathbf{r}_1 - \mathbf{r}', t_1 - t', \mathbf{R} + \frac{1}{2}(\mathbf{r}' - \mathbf{r}_2), T + \frac{1}{2}(t' - t_2)\right) \quad (\text{D.5})$$

$$B(\mathbf{r}', t', \mathbf{r}_2, t_2) = B\left(\mathbf{r}' - \mathbf{r}_2, t' - t_2, \mathbf{R} + \frac{1}{2}(\mathbf{r}' - \mathbf{r}_1), T + \frac{1}{2}(t' - t_1)\right) \quad (\text{D.6})$$

and for the convolution

$$C(\mathbf{r}_1, t_1, \mathbf{r}_2, t_2) = \int dt' \int d\mathbf{r}' A\left(\mathbf{r}_1 - \mathbf{r}', t_1 - t', \mathbf{R} + \frac{1}{2}(\mathbf{r}' - \mathbf{r}_2), T + \frac{1}{2}(t' - t_2)\right) \\ \times \left(\mathbf{r}' - \mathbf{r}_2, t' - t_2, \mathbf{R} + \frac{1}{2}(\mathbf{r}' - \mathbf{r}_1), T + \frac{1}{2}(t' - t_1)\right) \quad (\text{D.7})$$

A function can be expand as a Taylor Series as

$$f(x + \gamma) = e^{\gamma \partial_x} f(x), \quad (\text{D.8})$$

and employing it to Eq.(D.7)

$$C(\mathbf{r}_1, t_1, \mathbf{r}_2, t_2) = \int dt' \int d\mathbf{r}' e^{-\frac{1}{2}(\mathbf{r}_2 - \mathbf{r}') \cdot \nabla_{\mathbf{r}'}^B} e^{\frac{1}{2}(t' - t_2) \partial_{T'}^A} A\left(\mathbf{r}_1 - \mathbf{r}', t_1 - t', \mathbf{R}, T\right) \\ \times e^{-\frac{1}{2}(\mathbf{r}_1 - \mathbf{r}') \cdot \nabla_{\mathbf{r}'}^B} e^{-\frac{1}{2}(t_1 - t') \partial_{T'}^B} B\left(\mathbf{r}' - \mathbf{r}_2, t' - t_2, \mathbf{R}, T\right). \quad (\text{D.9})$$

Calling the function $\tilde{A} = A\left(\mathbf{r}_1 - \mathbf{r}', t_1 - t', \mathbf{R}, T\right) e^{-\frac{1}{2}(\mathbf{r}_1 - \mathbf{r}') \cdot \nabla_{\mathbf{r}'}^B} e^{-\frac{1}{2}(t_1 - t') \partial_{T'}^B}$ and $\tilde{B} = e^{-\frac{1}{2}(\mathbf{r}_2 - \mathbf{r}') \cdot \nabla_{\mathbf{r}'}^A} e^{\frac{1}{2}(t' - t_2) \partial_{T'}^A} B\left(\mathbf{r}' - \mathbf{r}_2, t' - t_2, \mathbf{R}, T\right)$

$$C(\mathbf{r}_1, t_1, \mathbf{r}_2, t_2) = \int dt' \int d\mathbf{r}' \tilde{A}\left(\mathbf{r}_1 - \mathbf{r}', t_1 - t', \mathbf{R}, T\right) \tilde{B}\left(\mathbf{r}' - \mathbf{r}_2, t' - t_2, \mathbf{R}, T\right)$$

The integral has convolution form, therefore the Fourier Transform

$$C(\mathbf{p}, E, \mathbf{R}, T) = \mathcal{F}[\tilde{A} \star \tilde{B}] = \tilde{A}(\mathbf{p}, E, \mathbf{R}, T) \tilde{B}(\mathbf{p}, E, \mathbf{R}, T) \quad (\text{D.10})$$

where

$$\tilde{A}(\mathbf{p}, E, \mathbf{R}, T) \int_{-\infty}^{\infty} dt \int_{-\infty}^{\infty} d\mathbf{r} A(\mathbf{r}, t, \mathbf{R}, T) e^{-\frac{1}{2}(\mathbf{r} \cdot \nabla_{\mathbf{R}}^B + t \partial_T^B)} \quad (\text{D.11})$$

Using the property of the Fourier transform of a function with a phase

$$\mathcal{F}[e^{i\gamma \mathbf{r}} f(\mathbf{r})] = f(\mathbf{p} - a) \quad (\text{D.12})$$

According to equation (D.8)

$$f(\mathbf{p} - a) = e^{a \cdot \nabla_{\mathbf{p}}} f(\mathbf{p}) \quad (\text{D.13})$$

Therefore

$$\tilde{A}(\mathbf{p}, E, \mathbf{R}, T) = e^{\frac{i}{2}(\partial_T^B \partial_E^A - \nabla_{\mathbf{R}}^B \cdot \nabla_{\mathbf{p}}^A)} A(\mathbf{p}, E, \mathbf{R}, T) \quad (\text{D.14})$$

$$\tilde{B}(\mathbf{p}, E, \mathbf{R}, T) = e^{\frac{i}{2}(\nabla_{\mathbf{R}}^A \cdot \nabla_{\mathbf{p}}^B - \partial_T^A \partial_E^B)} B(\mathbf{p}, E, \mathbf{R}, T) \quad (\text{D.15})$$

The convolution in Wigner coordinates

$$C(\mathbf{p}, E, \mathbf{R}, T) = e^{\frac{i}{2} \left(\partial_T^B \partial_E^A - \partial_T^A \partial_E^B + \nabla_{\mathbf{R}}^A \cdot \nabla_{\mathbf{p}}^B - \nabla_{\mathbf{R}}^B \cdot \nabla_{\mathbf{p}}^A \right)} A(\mathbf{p}, E, \mathbf{R}, T) B(\mathbf{p}, E, \mathbf{R}, T) \quad (\text{D.16})$$

Before hand, we define the Fourier transform of a convolution in the Wigner coordinates by

$$C(\mathbf{p}, E, \mathbf{R}, T) = \int dt \int d\mathbf{r} e^{i(Et - \mathbf{p} \cdot \mathbf{r})} C(\mathbf{r}, t, \mathbf{R}, T) \quad (\text{D.17})$$

or

$$C(\mathbf{p}, E, \mathbf{R}, T) = \int dt \int d\mathbf{r} e^{i(Et - \mathbf{p} \cdot \mathbf{r})} C\left(\mathbf{R} + \frac{1}{2}\mathbf{r}, T + \frac{1}{2}t, \mathbf{R} - \frac{1}{2}\mathbf{r}, T - \frac{1}{2}t\right) \quad (\text{D.18})$$

One can write it, in a more compact and easy to manage form by taking the variables in Eqs.3.14 and 3.15 as shown in chapter 3.